

FRACTURE MODELING OF ASPHALT CONCRETE WITH HETEROGENEOUS
MICROSTRUCTURE

BY

JIAN WANG

A thesis submitted to the

Graduate School-New Brunswick

Rutgers, The State University of New Jersey

In partial fulfilment of the requirements

For the degree of

Master of Science

Graduate Program in Civil and Environmental

Engineering

Written under the Direction of

Hao Wang

And approved by

New Brunswick, New Jersey

[January 2015]

ABSTRACT OF THE THESIS

Fracture Modeling Of Asphalt Concrete With Heterogeneous Microstructure

by JIAN WANG

Thesis Director:

Hao Wang

Understanding fracture resistance of asphalt concrete is of great importance in designing pavements with long service life. This thesis focused on studying the micro and global fracture behavior of heterogeneous asphalt concrete with a numerical analysis approach. Finite element (FE) models were built with the capacity of taking heterogeneity into consideration. The asphalt concrete was modeled as a multi-phase material with coarse aggregates and fine aggregate matrix (FAM). Viscoelastic properties were assigned to the FAM. Different damage models were incorporated to study fracture at two length scales: micro-fracture within FAM and coarse aggregate-FAM interface under small displacement and global fracture resistance in the semi-circular bending (SCB) test.

For micro-fracture simulation, asphalt mixture was modeled with both adhesive and cohesive failure potential. Two different fracture models, cohesive zone model (CZM)

and extended finite element model (XFEM), were adopted to simulate fracture damage within the FAM (cohesive failure) and at the FAM-aggregate interface (adhesive failure), respectively. For global fracture properties, the SCB test was simulated to predict the crack propagation pattern and the load-crack mouth opening displacement (CMOD) curve of asphalt concrete. Parametric studies with different material properties of FAM and coarse aggregates-FAM interface, morphological characteristics of coarse aggregates, and testing conditions (loading rate and temperature) were carried out to study their effects on fracture behavior of asphalt concrete.

The numerical models provide an effective method to study fracture mechanism of heterogeneous asphalt concrete and generates meaningful findings. The development of cracking shows that the damage in the FAM material would initiate first at a small displacement and then interconnect with the damage developed at the FAM-aggregate interface. The higher angularity and larger aggregate size induces the greater damage level; while the orientation angle along with aspect ratio has influence on the anisotropic behavior of asphalt concrete. On the other hand, the SCB test simulations show good agreements with experimental results in the literature. Increasing fracture strength and energy of FAM significantly improves fracture resistance of asphalt concrete. The spatial distribution and angularity of coarse aggregate affect crack path; while the gradation and size of coarse aggregate affect fracture strength of asphalt concrete.

ACKNOWLEDGEMENT

Foremost, I would like to express my sincere gratitude to my advisor Dr. Hao Wang for the continuous support of my Master's study and research, for his patience, motivation, enthusiasm, and immense knowledge. His guidance helped me in all the time of research and writing of this thesis.

Besides my advisor, I would like to thank the rest of my thesis committee: Dr. Gucunski and Dr. Yong, for their encouragement, insightful comments, and hard questions.

I thank my fellow friends in our research group: Jiaqi Chen, Maoyun Li, Guangji Xu, Zilong Wang and Yangmin Ding. Their friendship helped me through the hard times during these two years. I thank Jiaqi Chen especially here for the help he offered me and the discussions we had together.

Last but not the least; I would like to thank my father Jinghe Wang who passed away in 2009, for raising me up as a single parent and teaching me the right attitude to thrive in this world. Without my father, I would not be standing where I am today.

TABLE OF CONTENT

ABSTRACT OF THE THESIS	ii
ACKNOWLEDGEMENT	iv
CHAPTER 1. INTRODUCTION	1
1.1 Introduction	1
1.2 Objectives	3
1.3 Research Approach	4
1.4 Organization of Thesis	6
CHAPTER 2. BACKGROUND REVIEW	7
2.1 Generation of Asphalt Concrete Microstructure	7
<i>2.1.1 Generation of Asphalt Concrete Microstructure using Digital Analysis</i>	7
<i>2.1.2 Generation of Asphalt Concrete Microstructure using Random Generation Method</i>	8
2.2 Fracture Mechanics Theories	9
<i>2.2.1 Linear Elastic Fracture Mechanics</i>	9
<i>2.2.2 Cohesive Zone Model</i>	10
<i>2.2.3 Extended Finite Element Method</i>	11
2.3 Anisotropy in Asphalt Concrete Performance	12
CHAPTER 3. MICROMECHANICAL ANALYSIS OF ASPHALT MIXTURE	
FRACTURE	14
3.1 Generation of Microstructure of Asphalt Mixtures	14
3.2 Theoretical Background	16
<i>3.2.1 Viscoelastic Model for FAM</i>	16
<i>3.2.2 Cohesive Zone Model at FAM-Aggregate Interface</i>	17
<i>3.2.3 XFEM for Crack Development in FAM</i>	19
3.3 Model Geometry and Parameters	21
3.4 Model Results and Analysis	24
<i>3.4.1 Crack Initiation</i>	24
<i>3.4.2 Cohesive and Adhesive Failure</i>	29
3.5 Parametric Study of Fracture Potential	33
<i>3.5.1 Effect of Loading Rate</i>	33
<i>3.5.2 Effect of FAM Modulus</i>	34

3.5.3 <i>Effect of Interface Bonding Properties</i>	35
3.5.4 <i>Effect of Interface Thickness and Modulus</i>	38
3.6 Aggregate Morphology	40
3.7 Analysis on Anisotropic Damage in Asphalt Concrete	43
3.8 Parametric Study of Damage Anisotropy	46
3.8.1 <i>Effect of Aggregate Angularity</i>	46
3.8.2 <i>Effect of Aspect Ratio and Orientation Angle</i>	49
3.8.3 <i>Effect of Maximum Aggregate Size</i>	53
3.9 Summary	56
CHAPTER 4. FRACTURE SIMULATION OF ASPHALT CONCRETE IN SEMI-CIRCULAR BENDING TEST	58
4.1 Finite Element Model of SCB Test	58
4.2 Model Validation with Experimental Results	60
4.3 Parametric Study	64
4.3.1 <i>Effect of Temperature and Loading Rate</i>	64
4.3.2 <i>Effect of Aggregate Spatial Distribution</i>	67
4.3.3 <i>Effect of Aggregate Angularity</i>	69
4.3.4 <i>Effect of Aggregate Gradation and Size</i>	71
4.3.5 <i>Effect of Fracture Parameters of FAM</i>	73
CHAPTER 5. CONCLUSIONS AND FUTURE WORK	76
5.1 Findings on Micromechanical Analysis of Asphalt Mixture Fracture	76
5.2 Findings on Microstructure-Induced Anisotropy in Damaged Asphalt Concrete	77
5.2 Findings on Simulation of Asphalt Concrete in Semi-Circular Bending Test	78
5.3 Recommendation for Future Work	79
REFERENCE	81

CHAPTER 1. INTRODUCTION

1.1 Introduction

Cracking is one of major causes of asphalt pavement deterioration at low and intermediate temperatures. Cracks significantly reduce the lifespan of pavements and increase maintenance and repair costs. Understanding cracking mechanism of asphalt mixtures is crucial for developing a mechanistic-based design method for asphalt pavements. Asphalt mixture is a heterogeneous multi-phase material including aggregate, binder, air void, and other additives. The overall fracture performance of asphalt mixture is dependent on the properties of each component, such as the moduli of asphalt binder and aggregate, binder viscosity, and the bonding condition between aggregate and asphalt. Other factors like the gradation, shape, angularity, and texture of aggregates also affect the fracture behavior of asphalt mixture (*Guddati et al. 2002, Sadd et al. 2004*). Therefore, a fracture model that can consider the microstructure of asphalt mixture is needed to accurately predict the fracture behavior of asphalt mixture and evaluate the effect of each mixture component on the overall performance of asphalt mixture.

The micromechanics-based models are effective to evaluate the influence of each component of asphalt concrete on the global fracture behavior by considering their individual material property and interface characteristic. These models can connect the micro-scaled heterogeneous effect with the global scale performance and thus the effect of material heterogeneity, damage evolution, and anisotropy could be accounted for in evaluating the overall performance of asphalt concrete. Converting the analysis of a large-scale heterogeneous mixture into a small-scale heterogeneous sample is reasonable

to evaluate the performance of a large-scale mixture or structure, since the selected sample is sufficient to represent the behavior of the large-scale body. This small-scale sample is typically referred to as the Representative Volume Element (RVE). Micromechanics-based model can be implemented with existing computational techniques to study the properties such as viscoelasticity and fracture behavior of material with high heterogeneity and complex geometry.

Even though a number of studies have been done to investigate the fracture performance of asphalt concrete using computational models, some factors affecting the fracture behavior of asphalt concrete have not been yet evaluated due to the limitation of the existing models. Factors such as heterogeneity, bonding condition between different material components, anisotropy and aggregate morphology have not yet been fully understood. The difficulty of accounting for these factors lies in the complexity of heterogeneous microstructure modeling and the characterization of the interaction mechanism in the numerical model. A model that can accurately characterize the fracture behavior of asphalt concrete in both micro and global scale is needed. This thesis developed micromechanics-based numerical models that successfully characterized different damage mechanisms in fine aggregate matrix (FAM) and the FAM-aggregate interface. The semi-circular bending (SCB) test simulation with heterogeneous microstructure accurately replicated the test result and studied the heterogeneous effect on the global scale. The study of this thesis offers better understanding of fracture performance of asphalt concrete and how the characteristics of each material component affects the global performance, which will ultimately lead to a better design of asphalt pavements.

1.2 Objectives

The objective of this study is to develop a numerical model to study the micro and global fracture behavior of heterogeneous asphalt concrete. In order to achieve this objective, the following research tasks were conducted:

- 1) Develop a numerical model for fracture simulation of asphalt mixtures with heterogeneous microstructure. The two-dimensional (2-D) microstructure models of asphalt mixtures were randomly generated with polygon shaped aggregates using a “take-and-place” approach. Asphalt mixture was modeled as a heterogeneous material with fine aggregate matrix (FAM), coarse aggregate, and the interface between FAM and aggregate. FAM was modeled as a viscoelastic material, while aggregate was modeled as a linear elastic material. Two different fracture models, cohesive zone model (CZM) and extended finite element model (XFEM), were adopted to simulate the fracture damage at the FAM-aggregate interface (adhesive) and within the FAM (cohesive), respectively. The generated microstructure samples were tested with direct tension loading at different loading rates. Crack initiation and propagation patterns were analyzed for both adhesive and cohesive failure. Parametric studies were conducted to evaluate the effect of loading rate, FAM instantaneous modulus, and bonding properties on the fracture behavior of asphalt mixture.

- 2) Study the effect of aggregate morphology and size on the anisotropy of asphalt concrete with a numerical heterogeneous model. Each microstructure model was generated according to a set of certain parameters: aspect ratio, angularity index, gradation, and orientation angle. The generated microstructure samples were

tested under tension in two orthogonal directions. The fracture damage in the FAM and the FAM-aggregate interface were studied to investigate the anisotropic behavior of asphalt concrete under damaged condition. The parametric analyses regarding aspect ratio, angularity index, maximum aggregate size, and orientation angle were carried out in this study.

3) Develop a numerical model for simulating the SCB test in order to characterize the fracture behavior of asphalt mixtures at global scale. The finite element model was validated using the experimental measurements available in the literature. The fracture damage of asphalt mixtures at different loading rates and temperatures was analyzed. Parametric studies were conducted to investigate the effect of mixture components on the fracture behavior of asphalt mixture, such as the strength and fracture energy of FAM and the distribution pattern and shape of coarse aggregate.

1.3 Research Approach

To achieve the thesis objectives, first, a systematic set of theories is needed from the theory of viscoelasticity, microstructure generation theory to the fracture mechanics theories. Then numerical models need to be generated and meshed properly with the material data collected from reliable sources for numerical simulations. Lastly, case analyses need to be done to offer results and conclusions for future studies. Each phase of the study is shown in Figure 1-1.

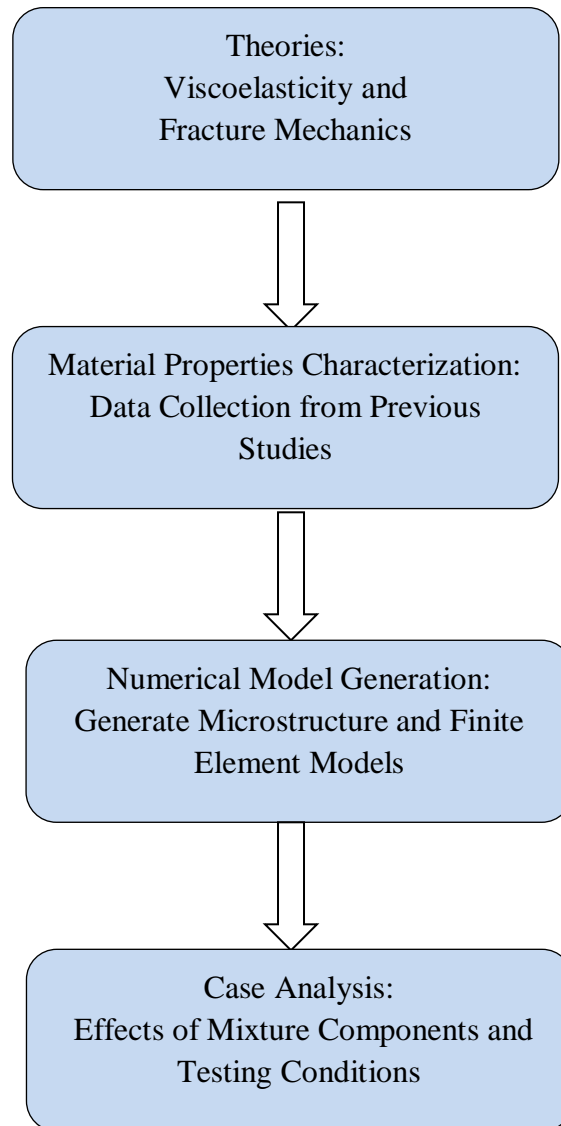


Figure 1-1 Flow Chart of Analysis Approach

1.4 Organization of Thesis

The first chapter briefly introduces the problem statement, thesis objectives, and research approach. The second chapter offers background review including previous studies done in microstructure model generation, theories of different fracture models, experimental and numerical fracture studies, etc. Chapter 3 describes the numerical heterogeneous model for cohesive and adhesive damage simulation and evaluates the effect of loading rate, FAM instantaneous modulus, bonding properties, and aggregate geometry on the fracture behavior of asphalt mixture. Chapter 4 describes the numerical simulation of the SCB test including validation of the numerical model and parametric analysis. Chapter 5 concludes the findings and offers suggestions for future research directions.

CHAPTER 2. BACKGROUND REVIEW

2.1 Generation of Asphalt Concrete Microstructure

2.1.1 Generation of Asphalt Concrete Microstructure using Digital Analysis

The digital image processing includes two steps: conversion from video pictures into digital form and applying mathematical procedures to obtain useful information from the picture. *Masad et al.* (1999) developed a system to characterize the internal structure of asphalt concrete using image analysis method. The equipment used for image analysis consisted of devices including image processing and analysis program, digital cameras and an X-ray tomography system for non-destructive imaging of the internal structure. The gray intensity in X-ray images was adopted as an indicator for different materials as each material corresponds to a certain gray intensity. A threshold gray value was chosen for identifying different materials such as air voids, asphalt binder and aggregates.

Digital image analysis has been used by many researchers (*Dai et al.* 2005, *Kim et al.* 2005, 2007, *Kim et al.* 2008, *Aragão et al.* 2010) to generate heterogeneous asphalt concrete microstructure models. The numerical model generated through this method has the same aggregate gradation and spatial distribution as the physical sample. Therefore, multiple specimens need to be scanned to reflect the variation of microstructure that is inherent for constructional materials such as asphalt mixture. This requires a specific set of equipment and extensive labor work to prepare and test the specimens in the laboratory.

2.1.2 Generation of Asphalt Concrete Microstructure using Random Generation Method

Random generation method generates microstructure models of asphalt mixtures according to a certain algorithm that considers the gradation and shape of aggregates. Regular shapes were used to represent the shape of aggregates by previous researchers: An elliptical particle model was used in analyzing the fracture behavior of random asphalt mixtures without considering the aggregate angularity effect (*Kristiansen et al. 2005*). A recent study was conducted to simulate the tension-induced fracture behavior of heterogeneous asphalt mixture using equilateral convex polyhedron to represent coarse aggregates, which simplified the geometry of aggregates by assuming the same length for the edges of aggregates (*Yin et al. 2012*). However, the regular-shaped aggregate model failed to characterize some mechanistic features such as stress concentration near the aggregate tip thus it is not a realistic representation of the actual aggregate shape.

Wang et al. (1999) proposed a take-and-place method for generating random aggregate structures for rounded and angular aggregates. The angular aggregates are generated with prescribed morphological parameters including aspect ratio and angularity index. This method is innovative in that it is the first time the shape of angular aggregates is controlled in a random microstructure generation algorithm. This method makes it possible to realistically characterize the mechanistic behavior due to aggregate geometry.

2.2 Fracture Mechanics Theories

2.2.1 Linear Elastic Fracture Mechanics

Fracture mechanics was developed during World War I by *Griffith* (1921) to explain the failure of brittle materials. *Irwin* (1957) improved Griffith's theory by introducing the role of plasticity in the fracture of ductile materials and he also established the concept of Stress intensity factor (SIF) and strain energy release rate to calculate the amount of energy available for fracture in terms of the asymptotic stress and displacement fields around a crack front in a linear elastic solid. One basic assumption in Linear Elastic Fracture Mechanics (LEFM) is small scale yielding where the size of the plastic zone is relatively small compared to the crack length, thus this theory is quite restricted. LEFM is only able to predict the stress state close to the crack tips of damaged bodies if the fracture process zone (FPZ) around the crack tip is very small.

Despite the restrictions, many numerical simulations are based on the LEFM theory. Some studies have evaluated the fracture toughness of asphalt mixtures using the J-integral concept or the stress intensity approach (*Mobasher et al. 1997; Mull et al., 2002; Kim et al., 2003*). Using the LEFM theory in finite element method requires refinement of the mesh near crack tip and the mesh needs to be updated once the crack propagates along. LEFM is not ideal in modeling the crack propagation in heterogeneous models considering the complexity of crack propagation route and the amount of remeshing work needs to be done.

2.2.2 Cohesive Zone Model

The Cohesive Zone Model (CAM) regards fracture formation as a gradual phenomenon in which the separation involving in the crack takes place across an extended crack tip or cohesive zone and is restricted by cohesive tractions. The cohesive zone model was developed based on the concepts proposed by *Barenblatt (1962)* and *Dugdale (1960)*. Compared to the LEFM, the cohesive zone method has the following advantages:

- Able to predict the behavior of uncracked structures accurately.
- The Size of the nonlinear zone does not need to be significantly small compared to the geometry of the whole model.
- Does not require an initial crack for the simulation process.

With the above advantages, the cohesive zone model is sufficient to model both brittle and ductile fractures which are observed in asphalt concrete pavements. Moreover, it can also be implemented with computational methods like finite element method and discrete element method. Many researchers used CZM to conduct numerical analysis (*Song et al., 2006; Kim et al., 2007; Kim et al., 2009*). Most importantly, it is a powerful tool to model bi-material interface especially when the material interface can be pre-defined. In the asphalt mixture, the weak areas that are most prone to cracking are usually the binder-aggregate interface. Previous studies have successfully utilized CZM to predict the fracture behavior along the mastic-aggregate interface (*de Souza et al. 2004, Soares et al. 2003, Souza et al. 2012, Kim et al. 2013*). However, it has been reported that convergence difficulty is usually accoutered when the crack path is not pre-defined and a large amount of CZM elements need to be embedded in the potential fracture area.

2.2.3 Extended Finite Element Method

The Extended Finite Element Method (XFEM) is a numerical technique based on the generalized finite element method and partition of the unity method (*Babuska and Melenk, 1997*). It was developed in 1999 by *Belytschko et al. (1999)*. It extends the classical finite element method by enriching the solution space to differential equations with discontinuous functions. It can adequately simulate the crack propagation without remeshing.

Recently, the extended finite element method (XFEM) has been used to model the crack propagation within the heterogeneous asphalt mixture (*Ng et al. 2011a,b, Saadeh et al. 2014, Lancaster et al. 2013*). The advantage of XFEM is that no pre-defined crack initiation and propagation path is needed. This means that crack can initiate and propagate depending on the stress distribution and the defined failure criteria. Compared to the cohesive zone method, the XFEM does not require the special element embedded at the element interface for crack development. However, it is difficult to simulate the interaction between the crack in the FAM material and the FAM-aggregate interface using the XFEM. Previous studies either use the same failure model at the FAM-aggregate interface and in the FAM material (*Ng et al. 2011a,b*) or neglect the heterogeneous nature of asphalt mixture (*Saadeh et al. 2014, Lancaster et al. 2013*).

2.3 Anisotropy in Asphalt Concrete Performance

Asphalt concrete is a composite material consisting of aggregates bonded with binder. Its internal structure is anisotropic due to the irregular aggregate and air void shape, orientation angles of aggregate particles and anisotropic compaction. The investigation and modeling of the anisotropic effect are considered necessary and have been conducted previously.

Underwood et al. (2005) conducted experimental tests to investigate the anisotropy in asphalt concrete and concluded that anisotropy contributes greatly on the behavior of asphalt concrete in compression but shows little effect on tensile properties. *Zhang et al. (2011)* included three test setup in his study to study the anisotropic viscoelastic properties of undamaged asphalt mixtures. His test results showed that all tested asphalt mixtures have significantly different tensile properties from compressive properties and asphalt mixtures exhibited anisotropic properties in compression. *Masad et al. (2002)* adopted a numerical micromechanics based approach to analyze the stiffness anisotropy in asphalt mixture and showed that the stiffness in horizontal direction was up to 30 percent higher than the stiffness in the vertical direction.

Chen et al. (2011) built a three-dimensional micromechanical model using discrete element method to investigate the stiffness anisotropy of asphalt concrete and their study showed that the stiffness of asphalt concrete was significantly dependent on the orientation of aggregate particles. *Wang et al. (2005)* conducted triaxial tests with cubical asphalt concrete specimens to characterize the anisotropic properties of asphalt concrete and it was discovered that there were obvious differences in vertical and horizontal direction. Many studies have been done to study the anisotropy in asphalt concrete under

undamaged condition (*Tutumluer et al. 2001; Seyhan and Tutumluer 2002*) and yet few have been done to analyze the anisotropic behavior considering the damaged condition.

CHAPTER 3. MICROMECHANICAL ANALYSIS OF ASPHALT MIXTURE

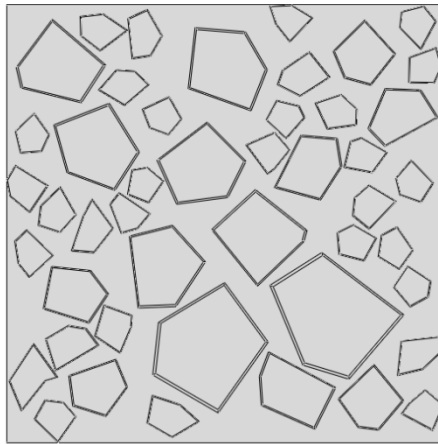
FRACTURE

3.1 Generation of Microstructure of Asphalt Mixtures

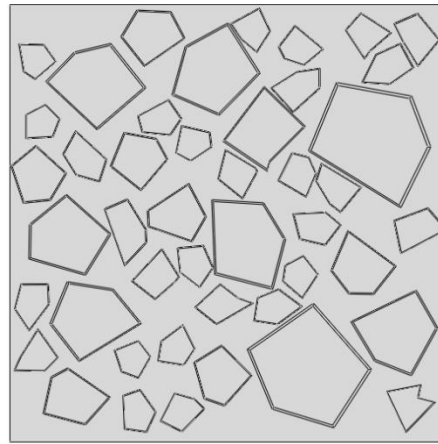
In order to predict the fracture behavior of asphalt mixtures, a numerical microstructure model is required to consider aggregate shape, size, and spatial distribution within the asphalt mixture. The predictive capabilities of numerical simulations directly rely on the accuracy of the microstructure model. This study modified the aggregate/inclusion generation algorithm that was originally proposed by *Wang et al. (1999)* by generating angular coarse aggregates as polygons with prescribed elongation ratios. The generation algorithm allows the number of aggregate edges vary from 4 to 10. After the shape and size of aggregate has been determined, the random aggregate structure is generated using a “take-and-place” approach (*Bazant et al. 1990, Wittmann et al. 1985 and De Scutter et al. 1993*). An aggregate particle having the largest size was first generated, and then placed randomly within the geometry boundaries. After the first take-and-place process, the process was repeated with a checking step that was used to prevent the second particle from overlapping with the first one. The above process was repeated until the aggregate particles coincide with the gradation curve. Since the particles are randomly generated, both concave and convex shapes can be generated. This random aggregate generation approach was tailored to model the interfacial zone surrounding the aggregate. A second boundary was generated around the aggregate to represent the binder film layer that has different fracture properties than the asphalt binder matrix.

Figure 3-1 shows five different microstructure models generated using the “take-and-place” approach. The aggregate gradation that was used to generate the microstructure of

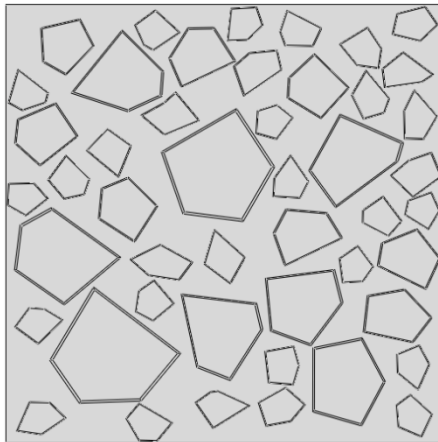
asphalt mixture is listed in Table 3.1 (*Sánchez-Leal, 2007*). The microstructure was generated by taking the aggregate size as a random variable uniformly distributed between adjoining sieve sizes. The width of the particle was defined to represent the size of the aggregate according to the definition used in sieving analysis. Pentagon was selected to represent the aggregate shapes in this study. The FAM-aggregate interface zone was generated with a thickness assumed to be five percent of the aggregate size (*Wang et al. 2013*).



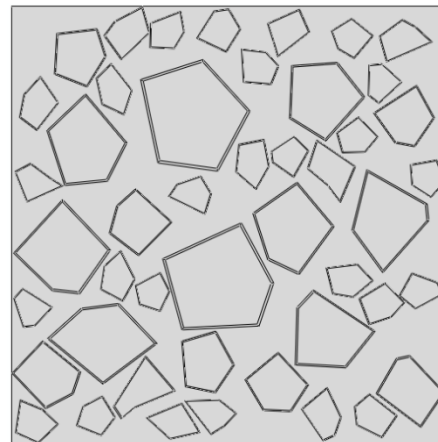
Sample # 1



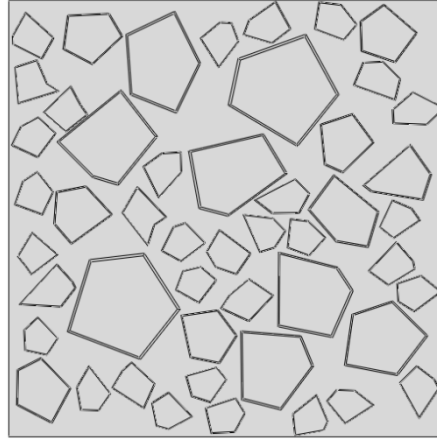
Sample # 2



Sample # 3



Sample # 4



Sample # 5

Figure 3-1 Microstructure of asphalt mixture from random generation**Table 3-1** Aggregate gradation for generation of microstructure (After Sánchez-Leal 2007)

	Sieve Size (mm)	Passing Percentage (%)
Coarse Aggregate	12.5	100
	9.5	90.9
	6.3	73.5
	4.75	62.5
Fine Aggregate	2.36	42
	1.18	28.4
	0.6	18.8
	0.3	12.5
	0.15	8.4
	0.075	5.7

3.2 Theoretical Background

3.2.1 Viscoelastic Model for FAM

The FAM material is a mixture of asphalt binder and fine aggregate (passing sieve size 4.75mm). It is modeled as a viscoelastic material to characterize the rate-dependent effect due to viscoelasticity of asphalt binder. Generalized Maxwell model (Maxwell-Wiechert

model) is widely used for viscoelastic materials like the asphalt mixture (*Tschoegl 1989*). The relaxation modulus can be plotted as a function of time and Prony series fit the data efficiently. The Prony series of the relaxation modulus can be expressed as:

$$G(t) = G_{\infty} + \sum_{i=1}^n G_i \exp(-t/\rho_i) \quad (3.1)$$

Where, G_{∞} , G_i , ρ_i and n are long-term equilibrium modulus, spring constants in the generalized Maxwell model, relaxation time and number of Maxwell unites in the generalized Maxwell model respectively.

An alternative form can be expressed with instantaneous modulus G_0 :

$$G(t=0) = G_0 = G_{\infty} + \sum_{i=1}^n G_i \quad (3.2)$$

Therefore,

$$G(t) = G_0 - \sum_{i=1}^n G_i [1 - \exp(-t/\rho_i)] \quad (3.3)$$

This form is more convenient when specifying the elastic properties separately from the viscous properties (Ferry 1980, ABAQUS 2010).

3.2.2 Cohesive Zone Model at FAM-Aggregate Interface

The cohesive zone model (CZM) with linear softening was used to simulate the adhesive fracture behavior at the FAM-aggregate interface. Cohesive elements represent the FAM-aggregate interface with a finite small thickness. The traction-separation law was used to define the constitutive response of the interface. The cohesive elements behave linearly until the damage initiation threshold is reached and then damage evolution follows. The maximum nominal stress criterion was adopted here to control the damage initiation in

the cohesive elements (Hillerborg 1976). This criterion assumes that damage will initiate when the maximum nominal stress ratio reaches one and it can be expressed as:

$$\max \left\{ \frac{\langle t_n \rangle}{t_n^o}, \frac{t_s}{t_s^o}, \frac{t_t}{t_t^o} \right\} = 1 \quad (3.4)$$

Where, t_n^o , t_s^o , t_t^o represent the peak values of the nominal stress when the deformation is either purely normal to the interface or purely in the first or second shear direction; and t_n , t_s , t_t are nominal traction stresses in three directions, respectively.

After the damage initiation criterion is reached, fracture damage evolves as the material stiffness degrades. A scalar variable D represents the overall damage of the cohesive element. The value of D varies from 0 to 1. The stress components within the cohesive element are affected by the damage variable D as below:

$$\begin{cases} t_n = \begin{cases} (1 - D)\bar{t}_n, & \bar{t}_n \geq 0 \\ \bar{t}_n & \text{(no damage under compression)} \end{cases} \\ t_s = (1 - D)\bar{t}_s \\ t_t = (1 - D)\bar{t}_t \end{cases} \quad (3.5)$$

Where, \bar{t}_n , \bar{t}_s , \bar{t}_t are stress components when there is no damage within the cohesive element.

Several damage evolution models can be used to define the damage variable D . Here the power law form was used. This criterion offers a power law interaction of fracture energies in three directions to evaluate the degradation under the mixed mode condition.

It can be expressed as:

$$\left\{ \frac{G_n}{G_n^c} \right\}^\alpha + \left\{ \frac{G_s}{G_s^c} \right\}^\alpha + \left\{ \frac{G_t}{G_t^c} \right\}^\alpha = D \quad (3.6)$$

Where, G_n , G_s and G_t are the work done by the traction force and its displacement in the normal and two shear directions, respectively; G_n^c , G_s^c and G_t^c are the critical fracture energies specified according to the material properties; and α is the power to be specified for this criterion (α is set as 1 in this study).

The damage evolutions model determines the softening behavior after damage initiation occurring in the fracture process zone. The softening region of the traction separation curve changes to a nonlinear shape when the parameter α is not equal to 1. The power law cohesive model becomes a bilinear cohesive model when α is equal to 1. The bilinear cohesive model has been proven to be an effective model to predict mix-mode crack propagation in the asphalt mixture (Song *et al.* 2006).

3.2.3 XFEM for Crack Development in FAM

An extended finite element method (XFEM) with virtue crack closure technique (VCCT) was used to simulate the fracture behavior within the FAM material. The XFEM does not require a potential crack path and thus provides an ideal way of modeling crack initiation and propagation in the FAM without pre-defined failure locations. The XFEM is an extension of the conventional finite element method based on the concept of partition of unity, which allows local enrichment functions to be easily incorporated into a finite element approximation. The presence of discontinuities is ensured by the special enriched functions in conjunction with additional degrees of freedom (Belytschko *et al.* 1999). For the purpose of fracture analysis, the enrichment functions typically consist of the near-tip asymptotic functions that capture the singularity around the crack tip and a discontinuous function that represents the jump in displacement across the crack surfaces.

The crack initiates depending on the stress distribution in the FAM material. The nodal enrichment function method and phantom node method were used to enable the prediction of crack initiation and crack propagation without re-meshing (*Babuska and Melenk 1997, Osher and Fedkiw 2002*). The approximation for a displacement vector function with the partition of unity enrichment is shown in Equation 3.7.

$$u = \sum_{I=1}^N N_I(x) [u_I + H(x)a_I + \sum_{\alpha=1}^4 F_{\alpha}(x)b_I^{\alpha}] \quad (3.7)$$

Where, $N_I(x)$ are the usual nodal shape functions; u_I is the usual nodal displacement vector associated with the continuous part of the finite element solution; a_I is the nodal enriched degree of freedom vector; $H(x)$ is the associated discontinuous jump function across the crack surfaces; $F_{\alpha}(x)$ is the associated elastic asymptotic crack tip functions and b_I^{α} is the nodal enriched degree of freedom. The first term on the right-hand side is applicable to all the nodes in the model; the second term is valid for nodes whose shape function support is cut by the crack interior; and the third term is used only for nodes whose shape function support is cut by the crack tip.

The discontinuous jump function across the crack surfaces, $H(x)$, is given by:

$$H(x) = \begin{cases} 1 & \text{if } (x - x^*) \cdot n \geq 0, \\ -1 & \text{otherwise,} \end{cases} \quad (3.8)$$

Where, x is a sample (Gauss) point; x^* is the point on the crack closest to x ; and n is the unit outward normal to the crack at x^* ;

The asymptotic crack tip functions in an isotropic elastic material, $F_{\alpha}(x)$ is given by:

$$F_{\alpha}(x) = \left[\sqrt{r} \sin \frac{\theta}{2}, \sqrt{r} \cos \frac{\theta}{2}, \sqrt{r} \sin \theta \sin \frac{\theta}{2}, \sqrt{r} \sin \theta \cos \frac{\theta}{2} \right] \quad (3.9)$$

Where, (r, θ) is a polar coordinate system with its origin at the crack tip and $\theta = 0$ is tangent to the crack at the tip.

The crack initiation criterion used in the FAM material was consistent with the criterion used at the FAM-aggregate interface. The virtual crack closure technique (VCCT) was used to control the crack propagation in the FAM material. The VCCT assumes that the strain energy released when a crack is extended by a certain amount is the same as the energy required to close the crack. Here a power law form is used to model the mix model behavior (*Xie and Bivvers 2006*):

$$f = \left(\frac{G_I}{G_{IC}}\right)^{\alpha_m} + \left(\frac{G_{II}}{G_{IIC}}\right)^{\alpha_n} + \left(\frac{G_{III}}{G_{IIIC}}\right)^{\alpha_o} \quad (3.10)$$

Where, crack tip debonds when f reaches the value of 1.0; G_I , G_{II} and G_{III} are strain energy release rates in normal and two shear directions; G_{IC} , G_{IIC} and G_{IIIC} are critical energy release rates in normal and two shear direction; α_m , α_n and α_o are the power index for each component respectively (they are assumed to be 1 in this study).

3.3 Model Geometry and Parameters

Due to the viscoelastic properties of asphalt binder, asphalt mixtures have different failure modes at low and high temperatures. In this study, asphalt mixture samples are assumed to be tested at the low temperature so fracture is the predominant failure mode. The heterogeneous nature of asphalt mixture requires fracture parameters to be modeled locally. This means that the FAM-aggregate interface and FAM material should have different fracture parameters.

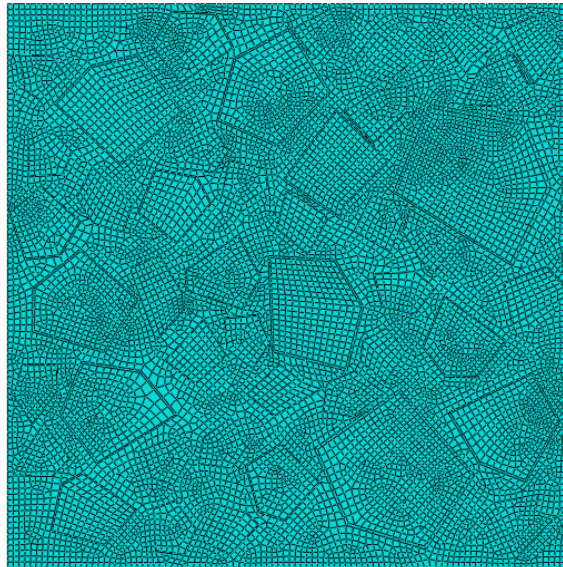
Experimental tests have been carried out to study the fracture properties of FAM and FAM-aggregate interface, respectively. Aragão *et al.* (2014) conducted two bending tests (semi-circular bending (SCB) and single-edge notched beam (SEB)) and one tension test (disk-shaped compact tension (DCT)) to characterize fracture properties of a fine aggregate mixture and provided the fracture properties at different temperatures. Khattak *et al.* (2007) studied mastic-aggregate adhesion and mechanistic characteristics of different asphalt mixtures by using the lap-shear test and tensile test with in-situ environmental scanning electron microscope. Fini *et al.* (2011) developed a blister test to study the mastic-aggregate fracture properties and estimated the interface strength and fracture energy. This study selected the fracture properties from previous researches to realistically build the computational model. The material parameters used in this study are listed in Table 3-2.

Table 3-2 Material properties of each mixture component at low temperatures

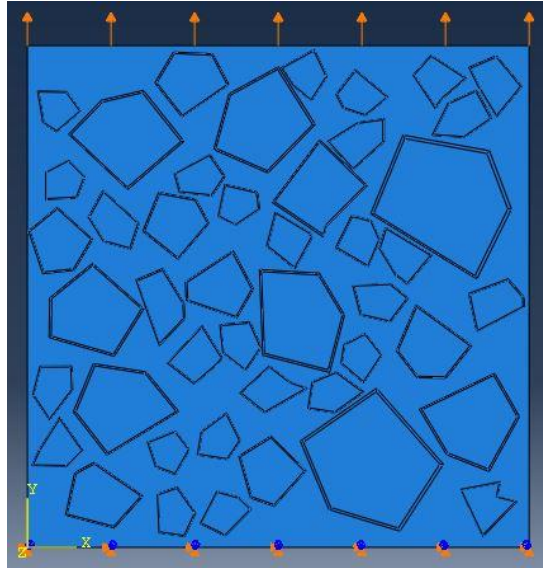
Aggregate		FAM-Aggregate Interface		Fine Aggregate Matrix				
Elastic Modulus	50 GPa	Elastic Modulus	50 GPa	Viscoelastic Prony series			Fracture Strength	Normal: 2.5MPa
		Fracture Strength	Normal: 0.5MPa	i	E _i (Pa)	τ _i (s)		1 st shear: 2.5MPa
			1 st shear: 0.5MPa	0	17.5E9	0		2 nd shear: 2.5MPa
		2 nd shear: 0.5MPa	1	6.79E9	1.13E-4	Critical Energy Release Rate	Normal: 200 J/m ²	
Fracture Energy	150 J/m ²	Normal: 150 J/m ²	2	5.51E9	3.14E-3		1 st shear: 600 J/m ²	
			3	3.03E9	1.3E-2			
		1 st shear: 450 J/m ²	4	1.44E9	1.64E-1			
			5	4.39E8	2.09			
2 nd shear:			6	1.87E8	37.7	2 nd shear: 600 J/m ²		
Poisson Ratio	0.15							

			450 J/m ²				
--	--	--	----------------------	--	--	--	--

The numerical simulations were conducted using the commercial finite element analysis package ABAQUS. Due to the high stress singularity at aggregate tip and the random distribution of aggregate within the asphalt mixture model, the free meshing method with mesh control was used. Mesh sensitivity analysis was conducted to assure the model accuracy. To have a balance between computational accuracy and time, an overall mesh seed size of 0.5mm was used to generate the mesh. The representative volume element (RVE) size selected here is a 50mm × 50mm square. It has the capacity of including at least two largest aggregates without significantly increasing the computational cost. An illustration of meshes is shown in Figure 3-2 (a). The numerical specimen was fixed at the bottom and the tension load was applied on the top surface, as shown in Figure 3-2 (b). A vertical displacement was applied to the model at a rate of 0.5mm/s.



(a)



(b)

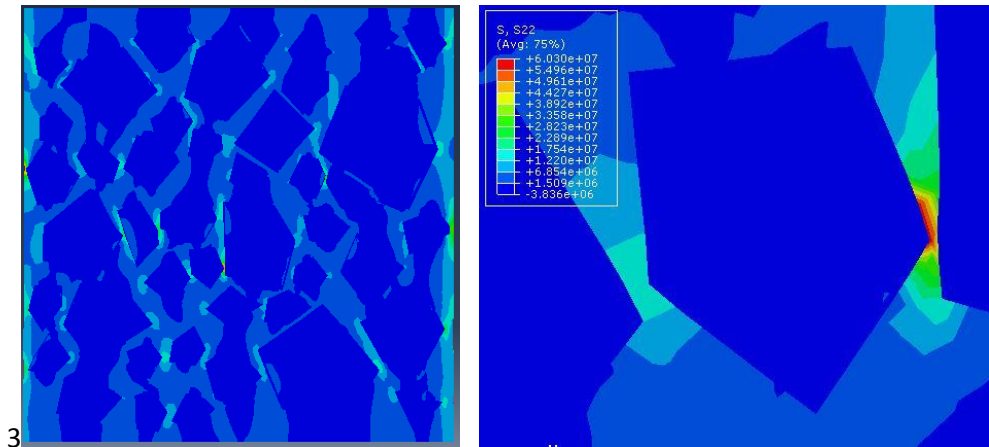
Figure 3-2: (a) Meshes of the finite element model and (b) boundary and loading condition (Sample #2 selected)

3.4 Model Results and Analysis

3.4.1 Crack Initiation

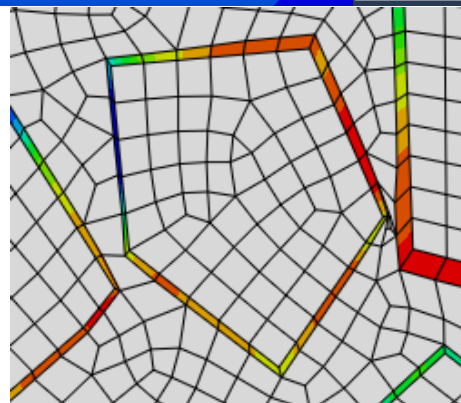
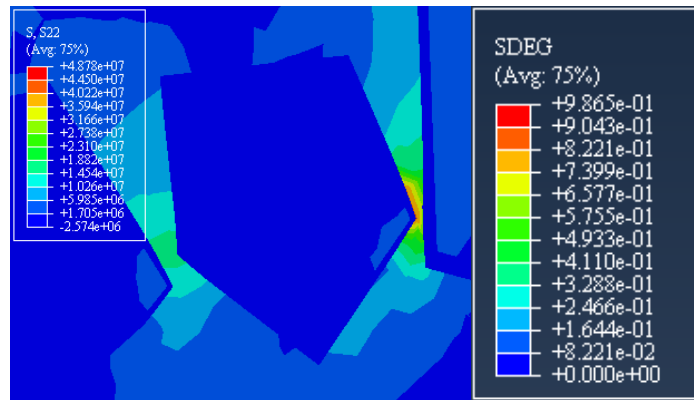
An intact model that only contains continuum elements and does not allow fracture development was first developed for comparison with the fracture model. Figures 3-3 (a), (b) and (c) compare the tensile stress distributions between the intact model, the fracture model with adhesive failure only, and the fracture model with cohesive and adhesive failure. The results from the intact model and the fracture model with adhesive failure only indicate that a very high level of stress concentrates near the aggregate tip that is close to another large aggregate tip. This indicates where fracture would initiate within the FAM material. On the other hand, in the fracture model with cohesive and adhesive failure, crack initiates in the FAM material along with the development of interface damage. The local strain energy is released to create new crack surfaces and the crack

initiation reduces the stress concentration. The damage along the FAM-aggregate interface results in lower stresses around the aggregate tip, compared to the intact model without crack potential.

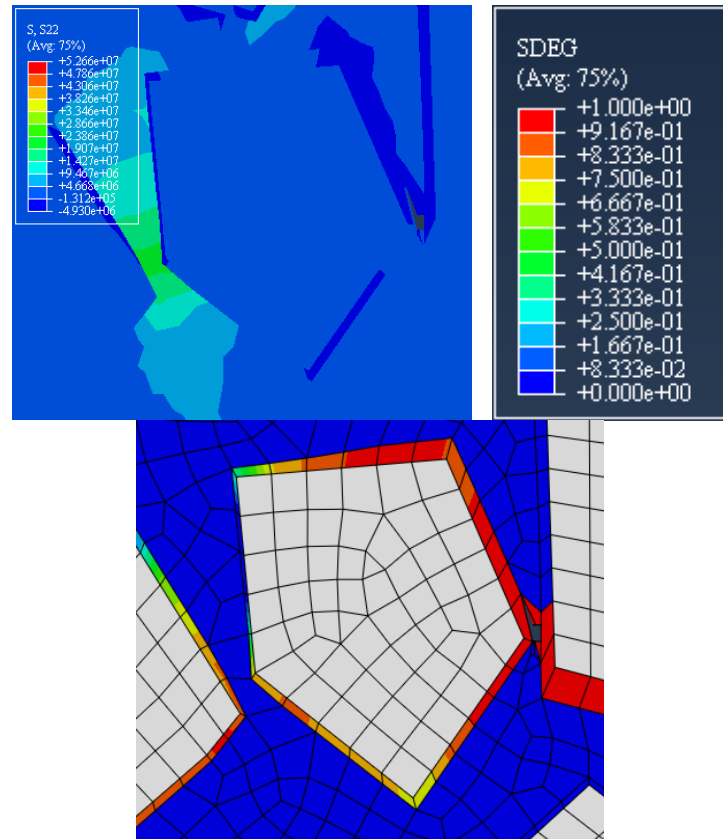


3

(a)



(b)



(c)

Figure 3-3 Tensile stress distribution and local damage for (a) the intact model without crack potential, (b) the model with adhesive failure only, and (c) the model with cohesive and adhesive failure

To study how the cohesive and adhesive failure develop under loading, two separate simulations were conducted: one allowed cracking to initiate and propagate at the FAM-aggregate interface (adhesive failure) and within the FAM material (cohesive failure); and the other one only allowed cracking to occur at the FAM-aggregate interface. The average values of stiffness degradation variable (SDEG) of four cohesive elements near the area where the crack in the FAM material initiates were compared between two models, as is shown in Figure 3-4. The SDEG indicates the adhesive failure of cohesive elements at the FAM-aggregate interface with a scale of 0-1. The SDEG value of one

indicates that the cohesive element is fully cracked. It shows that consideration of cohesive failure in the FAM material causes the adhesive failure at the FAM-aggregate interface to develop faster. Figures 3-5 (a), (b), (c), (d) and (e) show how the overall damage evolves at different displacements. The evolution of cracking failure shows that the damage in the FAM material would develop first at the small displacement and then interconnected with the damage developed at the mastic-aggregate interface. As the displacement keeps increasing, the interface adhesive damage is the dominant failure mode.

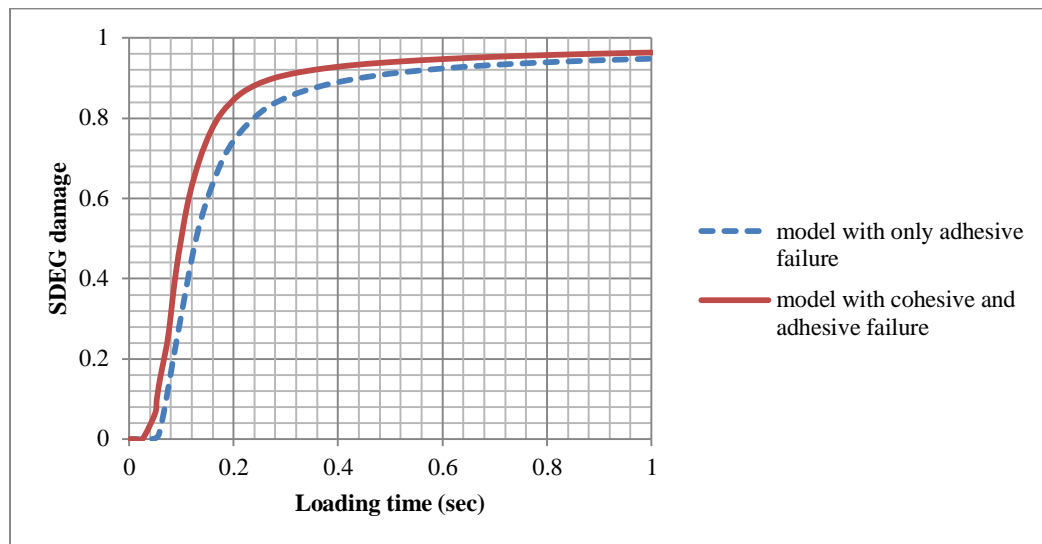
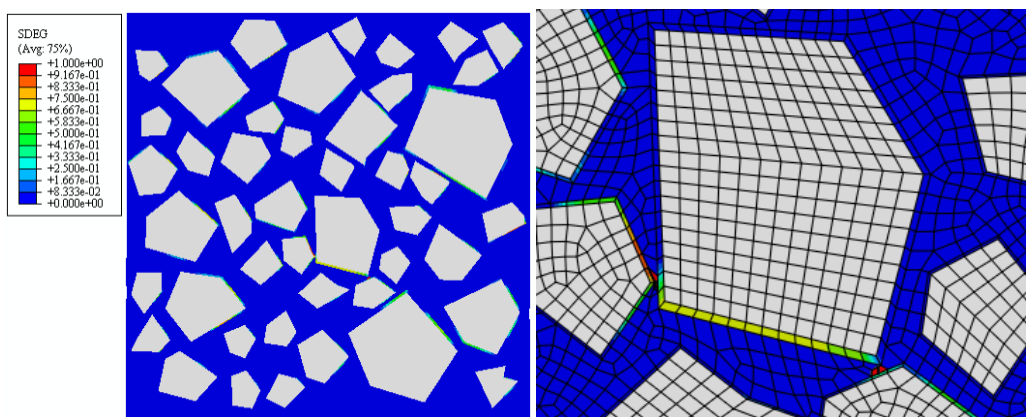
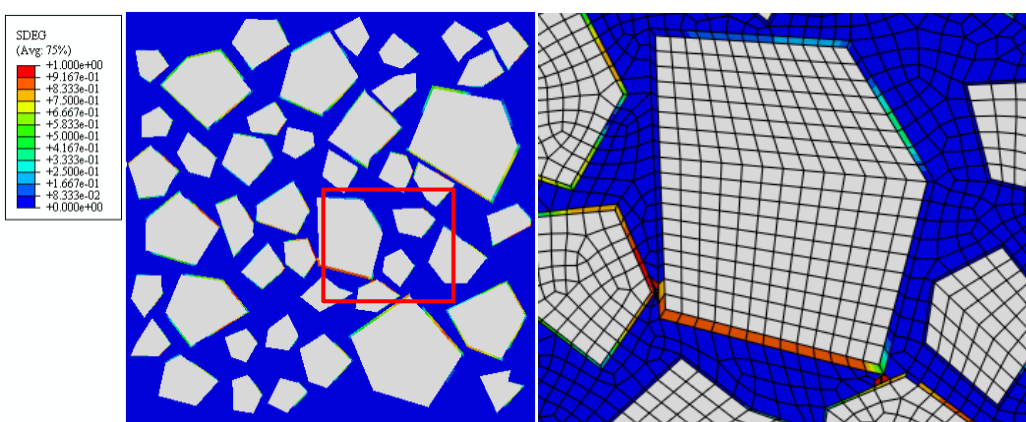


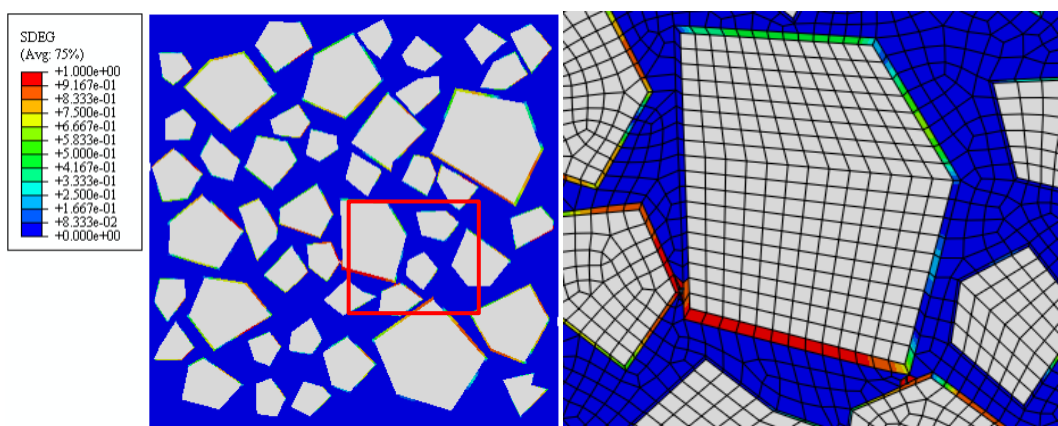
Figure 3-4 Average SDEG values of cohesive elements close to the crack in the FAM



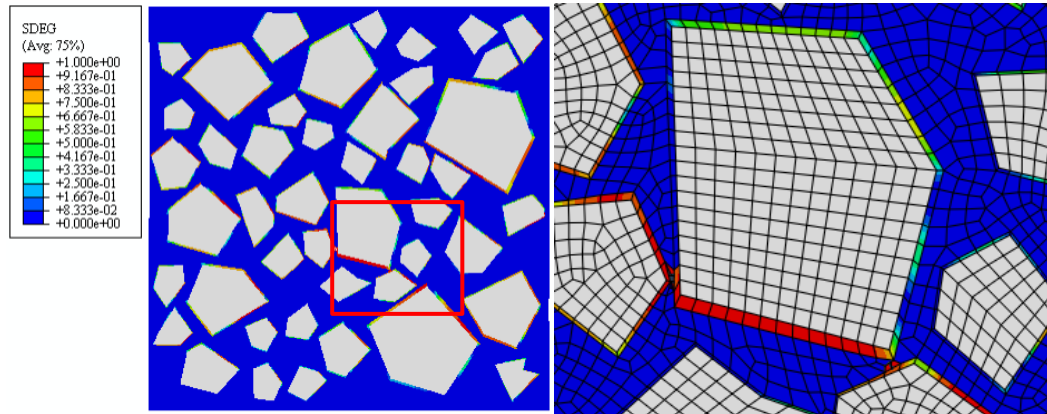
(a)



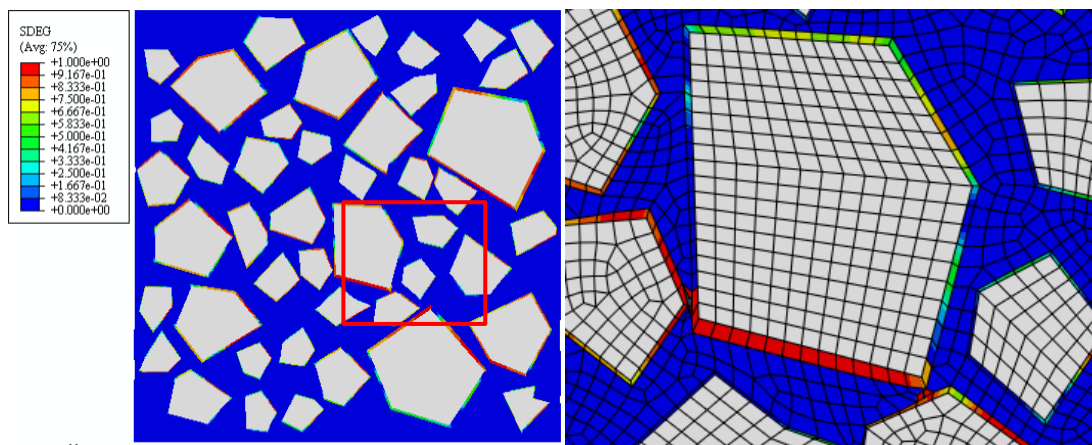
(b)



(c)



(d)



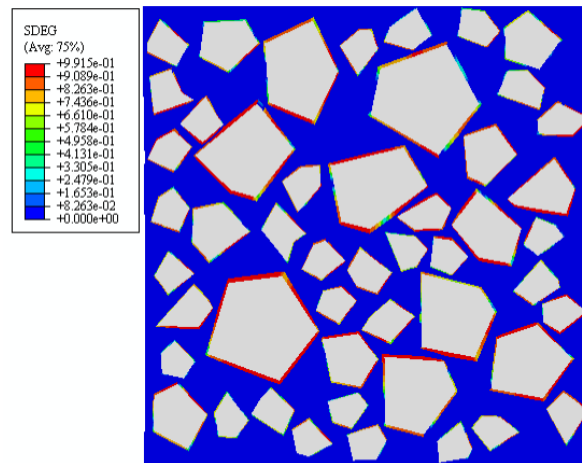
(e)

Figure 3-5 FAM-Aggregate interface damage at displacement of: (a) 0.1mm; (b) 0.2mm; (c) 0.3mm (d) 0.4mm; (e) 0.5mm.

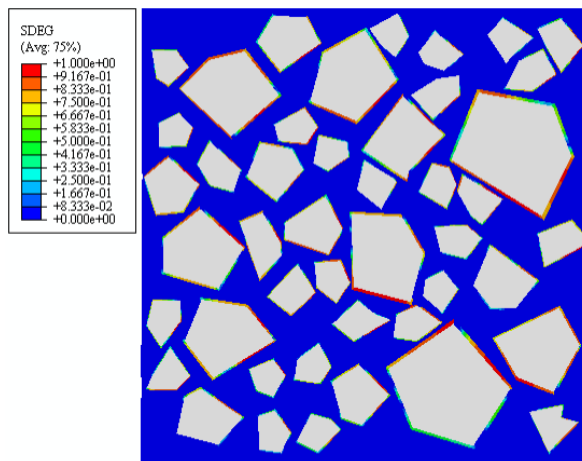
3.4.2 Cohesive and Adhesive Failure

The five microstructure samples that were randomly generated using the same aggregate gradation curve (as shown in Figure 3-1) were simulated using the same loading and boundary conditions. The damage maps of SDEG are shown in Figures 3-6 (a) – (e), respectively, for the five samples. The results show that most of the high SDEG values occur along the FAM-aggregate interface of large aggregates, although the specific distribution pattern of SDEG values varies with the microstructure of asphalt mixture.

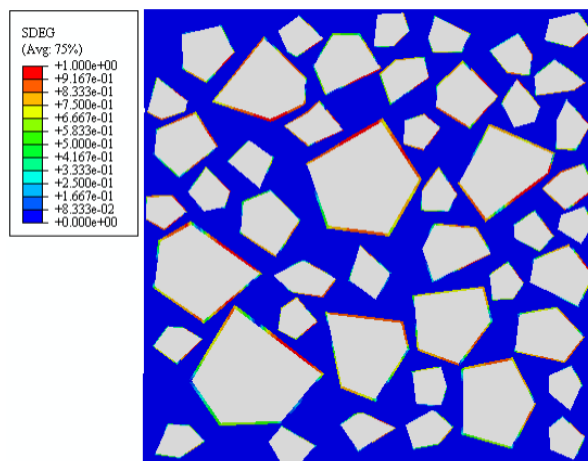
Figure 3-6 (f) plots the frequency distribution of SDEG values for the five samples. The frequency distributions of SDEG values of five samples have similar trends with two peak values occurring at 0 and 0.9. The means and standard deviations of SDEG values of five samples were found close to each other, as shown in Table 3-3. This indicates although the critical failure locations may vary depending on the microstructure of asphalt mixture, the global failure potential at the specimen level does not vary significantly with the randomly generated microstructure.



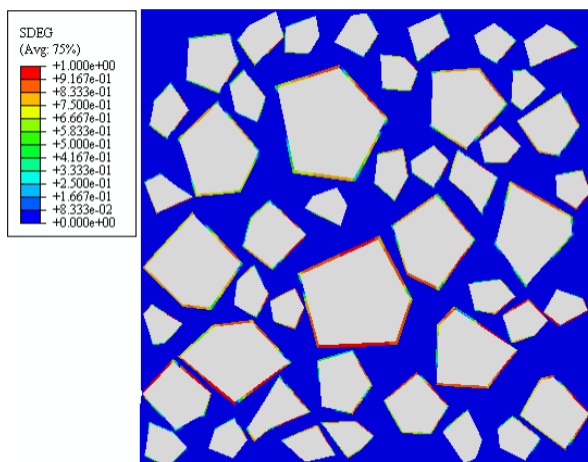
(a)



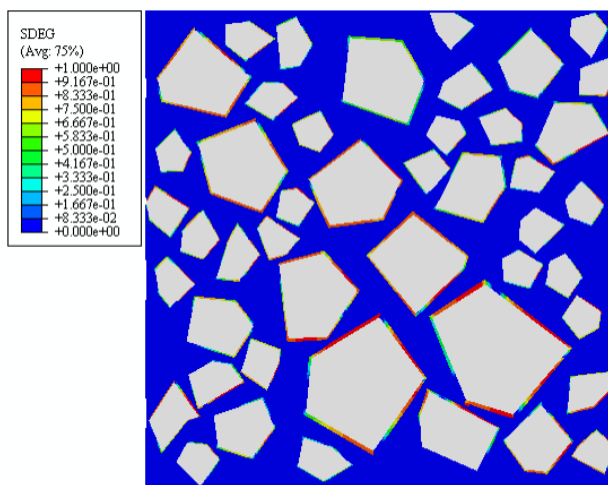
(b)



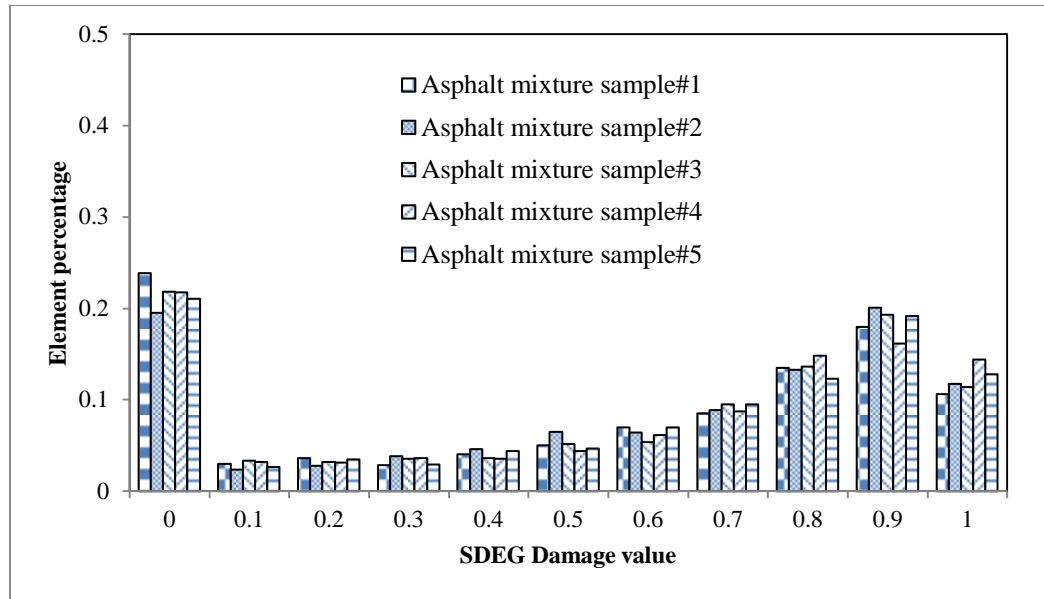
(c)



(d)



(e)



(f)

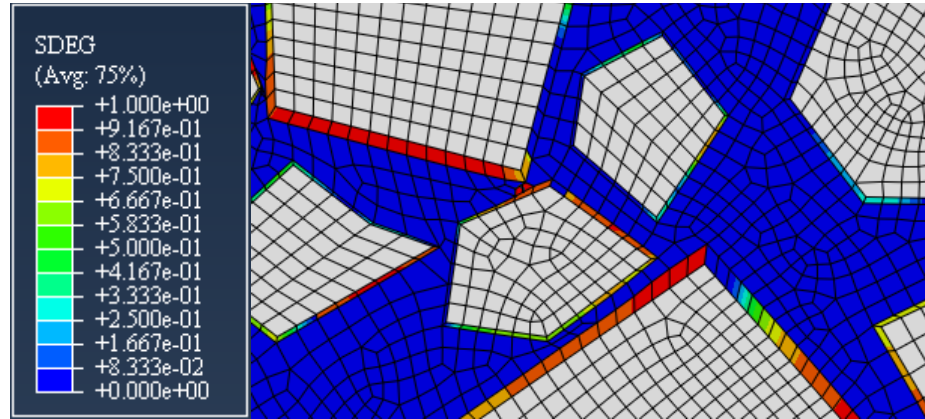
Figure 3-6 (a) - (e): SDEG maps; and (f) frequency distribution of SDEG values of five randomly generated samples.

Table 3-3 SDEG values of different samples

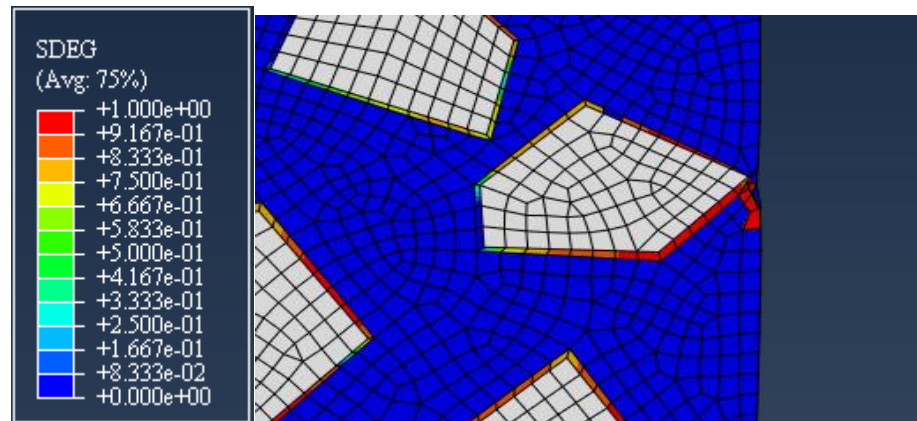
Sample#	Mean SDEG values	Standard deviation of SDEG values
1	0.499	0.355
2	0.534	0.343
3	0.517	0.354
4	0.522	0.356
5	0.527	0.352

Figures 3-7 (a) and (b) show two typical locations where the cohesive failure initiates in the FAM material as observed from the five samples. The critical locations were found in the area where an aggregate tip is close to the boundary of another aggregate (Figure 3-7(a)) or where an aggregate tip is close to the sample boundary (Figure 3-7(b)). Those locations are also within the area where the highest level of stress occurs in an intact model without crack development. This indicates that high aggregate angularity may

cause premature fracture failure if the binder content is not increased to meet the mix design criteria, although it provides skeleton structure to prevent shear-induced rutting.



(a)



(b)

Figure 3-7 Two typical crack initiation locations in FAM: (a) where a sharp aggregate tip is close to another aggregate boundary; (b) where a sharp tip is close to sample boundary

3.5 Parametric Study of Fracture Potential

3.5.1 Effect of Loading Rate

To quantify how the loading rates affect the fracture behavior, three different loading rates were applied: 0.5mm/min, 0.5mm/sec and 5mm/sec. The frequency distributions of SDEG values were plotted in Figure 8. The mean SDEG values of the asphalt mixture

samples are 0.573, 0.534 and 0.414, respectively, under 5mm/sec, 0.5mm/sec and 0.5mm/min loading rates. The peak of the frequency distribution curve shifts to a higher value as the loading rate increases. This indicates that the higher loading rates induce the greater fracture potential in the asphalt mixture. Viscoelastic properties of FAM material induce a rate-dependent effect on the overall mixture performance. The higher loading rate results in the greater modulus of FAM in the model. The higher modulus of FAM would induce more stress concentration at the interface layer between aggregate and FAM where the CZM was used. The greater stress concentration at the interface causes more fracture damage.

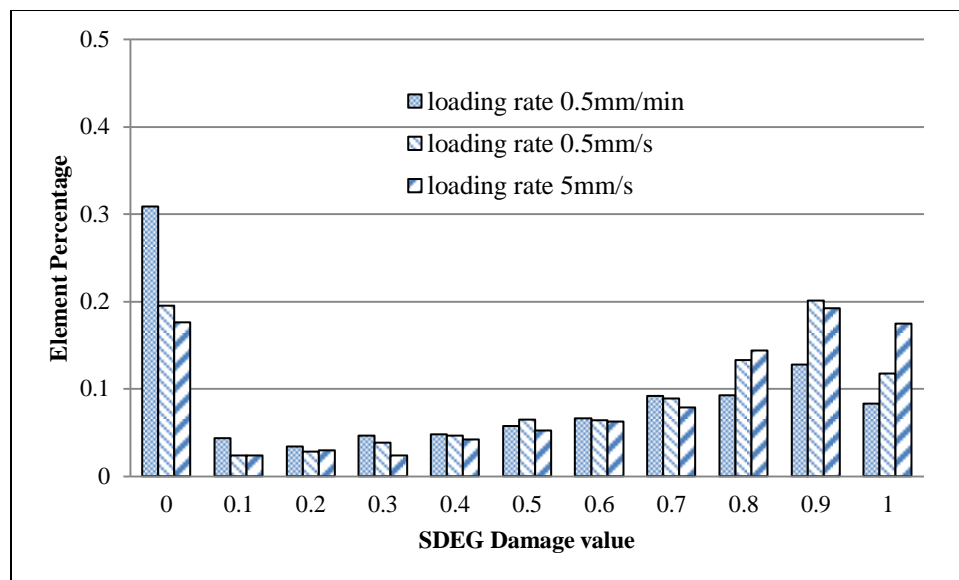


Figure 3-8 SDEG frequency distributions of the sample under different loading rates

3.5.2 Effect of FAM Modulus

One key parameter affecting the fracture behavior is the instantaneous modulus of the FAM material that is dependent on the performance grade of asphalt binder. The

instantaneous modulus (E_0) used in previous cases is 17.5GPa. To investigate how the FAM modulus affects the overall fracture behavior, $1/3 E_0$, $2/3 E_0$ and $4/3 E_0$ were assigned to the FAM material at the same loading rate (0.5mm/s). The frequency distribution curves of SDEG values were plotted in Figure 3-9, respectively, for different FAM moduli. It reveals that the higher modulus results in the higher damage level in the asphalt mixture, which is consistent with the results at different loading rates.

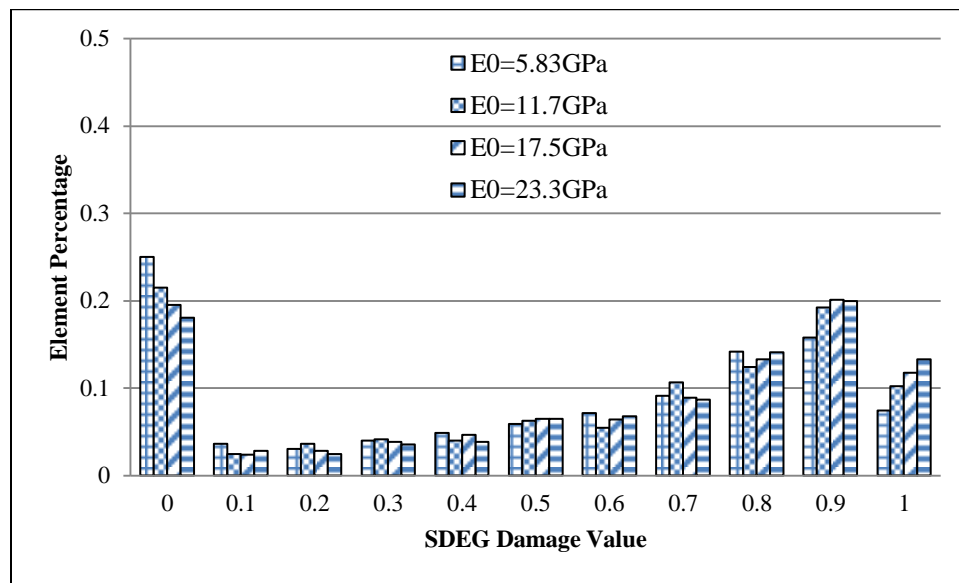
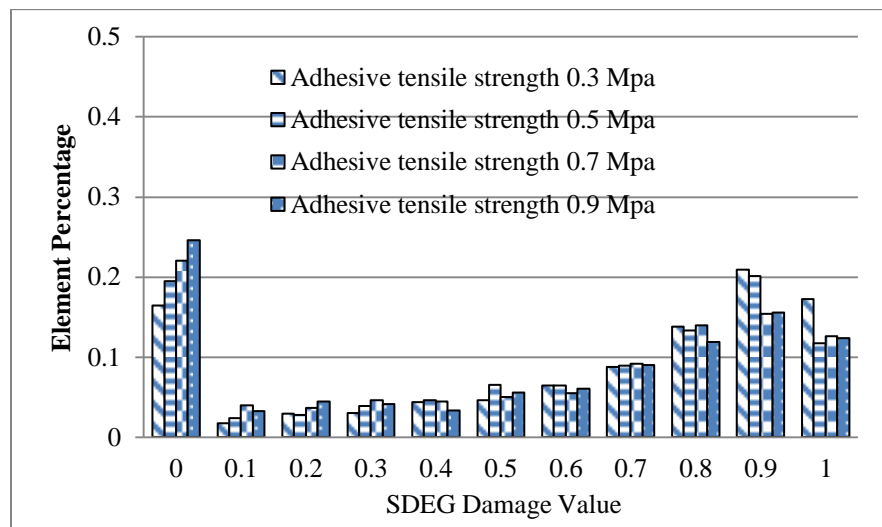


Figure 3-9 SDEG frequency distributions of samples with different E_0

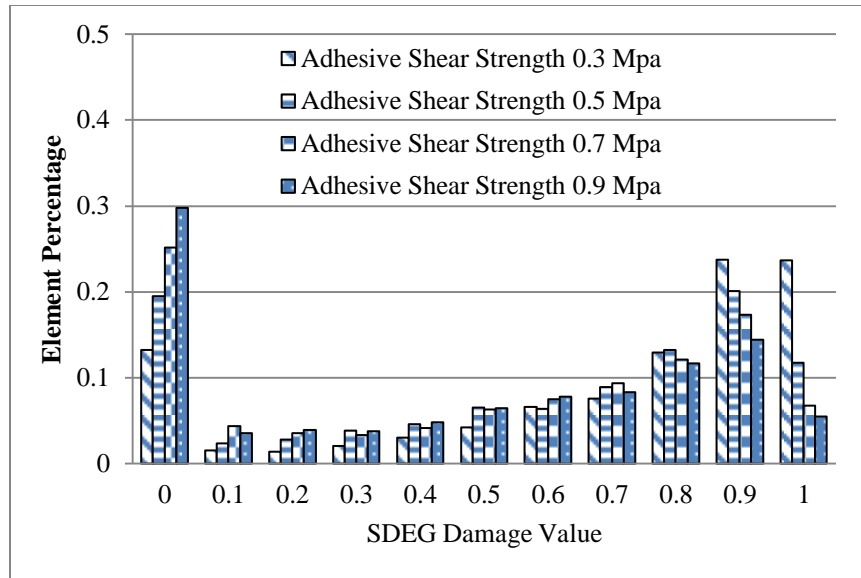
3.5.3 Effect of Interface Bonding Properties

The effect of fracture strength and fracture energy at the FAM-aggregate interface on the failure potential of asphalt mixture was analyzed. This analysis is necessary considering different interface conditions may exist in the reality. It has been found that the bonding between aggregate and asphalt binder is affected by the physical properties and chemical composition of aggregate, interfacial tension between binder and aggregate, temperature

and moisture conditions (Tarrer and Wagh 1991). Bonding strength and interfacial fracture energy were analyzed separately. The effects of bonding strength on fracture potential were shown in Figures 3-10 (a) and (b), respectively, for the tensile and shear adhesive strength. It was found that the adhesive shear strength has more significant effect on the fracture potential as compared to the adhesive tensile strength. As the adhesive strength changes from 0.9 to 0.3MPa, the mean SDEG values of the asphalt mixture samples changes from 0.485 to 0.585 for shear adhesive strength and from 0.421 to 0.648 for shear adhesive strength. This indicates that the failure at the aggregate-mastic interface could be more prone to shear failure due to the heterogeneous nature of asphalt mixture. It further emphasized the important influence of aggregate microstructure on fracture potential of asphalt mixture.



(a)



(b)

Figure 3-2 SDEG frequency distributions of samples with different adhesive (a) tensile and (b) shear fracture strength

Figure 3-11 shows the change of fracture potential as the fracture energy. The results show that the asphalt mixture fracture behavior is highly sensitive to the bonding strength at the FAM-aggregate interface as compared to the interfacial fracture energy. This indicates that bonding strength should be considered as an importance criterion in selection of raw material for asphalt mixture design. Bonding strength became the vital parameter for HMA fracture when applying a constant strain rate load. However, the interfacial fracture energy would be a key factor under the repeated load at a relatively small magnitude.

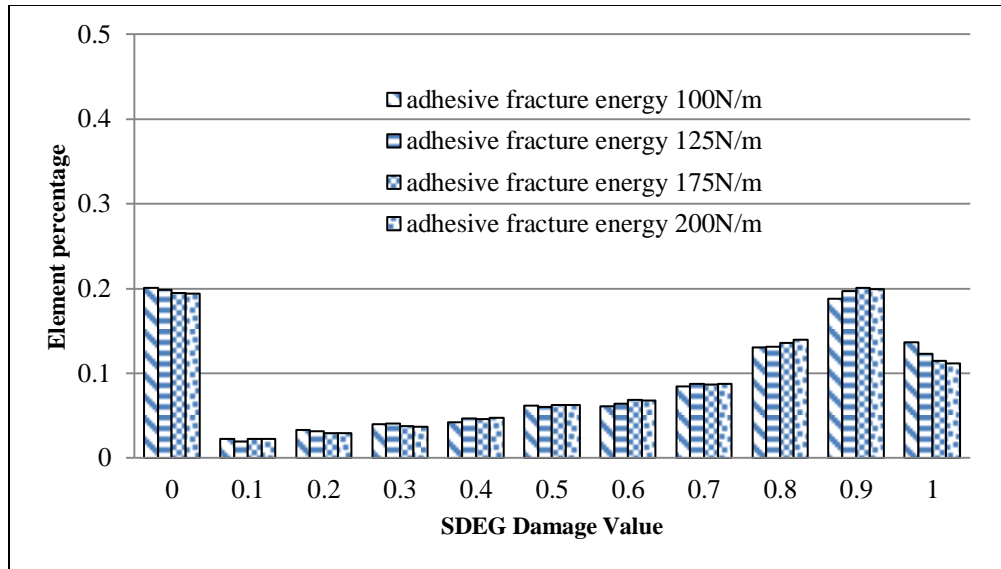


Figure 3-3 SDEG frequency distributions of samples with different adhesive fracture energy

3.5.4 Effect of Interface Thickness and Modulus

The thickness and modulus of the FAM-aggregate interface pose great significance on the fracture performance of asphalt concrete. Previous studies find that the binder film around the coarse aggregate show high elastic modulus when two aggregate particles are compacted close to each other (Wang *et al.* 2013) and the elastic modulus of the binder film gets significantly higher when it is aged (Allen *et al.* 2012, Tarefder *et al.* 2013). Hence a relatively high elastic modulus was selected in this study for the FAM-aggregate interface. The film thickness is also depending on the blending condition of fine aggregates and binder and the film modulus is affected by the level of aging in asphalt binder. To study the thickness influence, models with different interface thickness ratio (0.03, 0.05 and 0.08) and modulus (5GPa, 20Gpa and 50GPa) were built. The frequency distributions of SDEG values for different interface thicknesses are plotted in Figure 3-12. The average SDEG values are: 0.49, 0.51 and 0.53 for samples with the thickness ratio of

0.08, 0.05 and 0.03 respectively. The interface damage is sensitive to the film thickness. The thinner the interface layer, the higher the damage is when the three samples are subjected to the same displacement-controlled loading.

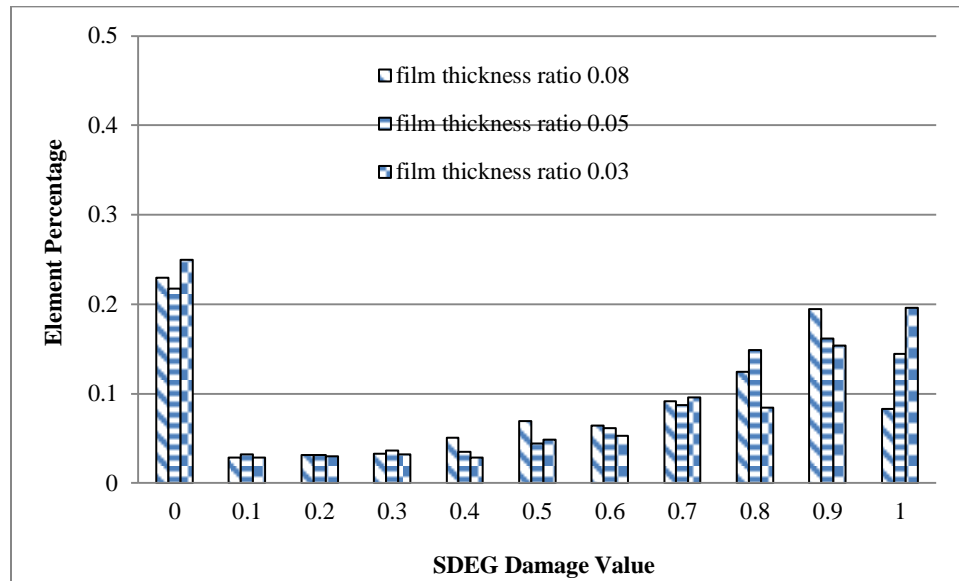


Figure 3-4 SDEG frequency distributions of samples with different film thickness ratio

Figure 3-13 shows the frequency distribution of SDEG values for each film modulus. When the interface modulus was equal to 5GPa, more than 90 percent of the interface area did not have damage under the tension. The damage level increased as the interface film modulus increased. The 5GPa case represents the situation for virgin asphalt binder; while the 50GPa case may represent the heavily aged binder. The highly aged asphalt concrete is more prone to interface fracture.

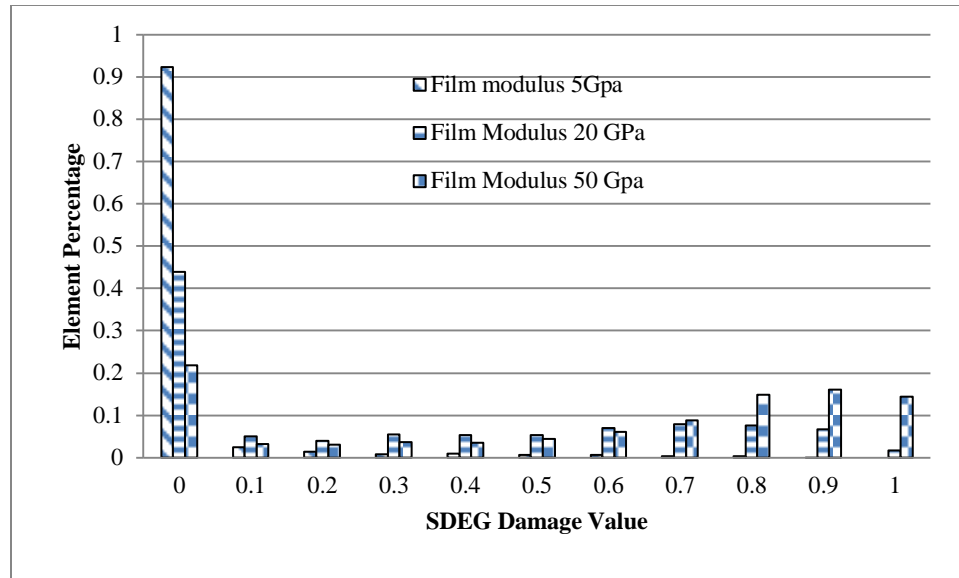


Figure 3-5 SDEG frequency distributions of samples with different film modulus

3.6 Aggregate Morphology

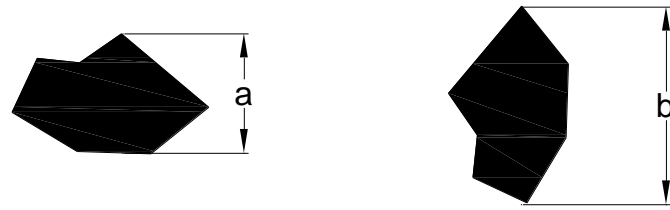
Imaging technology and image analysis have been used for aggregate morphology analysis. A number of studies have been carried out to quantify the morphological characteristics based on the imaging technology. Some researchers used direct linear dimensions, perimeters and areas to represent parameters such as shape, angularity and surface texture (*Brzezicki et al. 1999, Kuo et al. 1996*).

Meanwhile, additional measurements over the boundaries or processing of intensity signals have also been used to characterize shape, angularity and surface texture properties (*Wang et al. 2005, Masad et al. 2000*). *Rao et al. (2002)* described the aggregate angularity using the frequency distribution of the change in angles along the perimeter. *Wang et al. (2005)* analyzed the angularity of aggregates with Fourier analysis method, in which angularity was captured using harmonics with certain frequencies. *Masad et al. (2001)* developed a radius angularity index based on the difference between

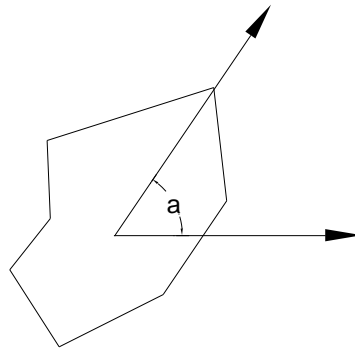
the radius of a particle in a certain direction and a radius of an equivalent ellipse taken in the same direction. By reviewing the previous studies on aggregate morphology, conclusions can be made that many indices were defined differently and the method used in each study were not the same.

One of the major indices to evaluate the shape of aggregates is aspect ratio, which is defined as the ratio of the major axis to the minor axis of a particle. Since a 2-D numerical model was adopted in this study, the aspect ratio was defined as the ratio between the longest aggregate dimension and the shortest aggregate dimension. Another parameter used to describe the aggregate shape properties is the form ratio. It has been found that there is a good correlation between form ratio and aspect ratio (*Masad et al. 2000*). In this study the aspect ratio was adopted as an index to represent the aggregate proportion. The polygon aspect ratio is defined as the ratio between the major axis and the minor axis, where the major axis is defined as the longest diagonal length of the polygon (“b” in Figure 3-14 (a)) and the minor axis is defined as the longest length in the direction perpendicular to the polygon major axis (“a” in Figure 3-14 (a)).

In addition, orientation angle is important in describing the spatial distribution of aggregate. It is defined as the angle between the long axis of the equivalent ellipse and the horizontal direction, as is shown in Figure 3-14 (b).



(a)



(b)

Figure 3-6 Schematic diagram of aggregate shape properties: orientation angle α and aspect ratio b/a .

Another important parameter in aggregate morphology is the particle angularity. In this study, the radius-based 2-D angularity index was used, as shown in Equation 3.11 (Masad *et al.* 2000). It measures the difference between a particle radius in a certain direction and that of an equivalent ellipse.

$$AI = \sum_{\theta=0}^n \frac{|R_{\theta} - R_{EE\theta}|}{R_{EE\theta}} \quad (3.11)$$

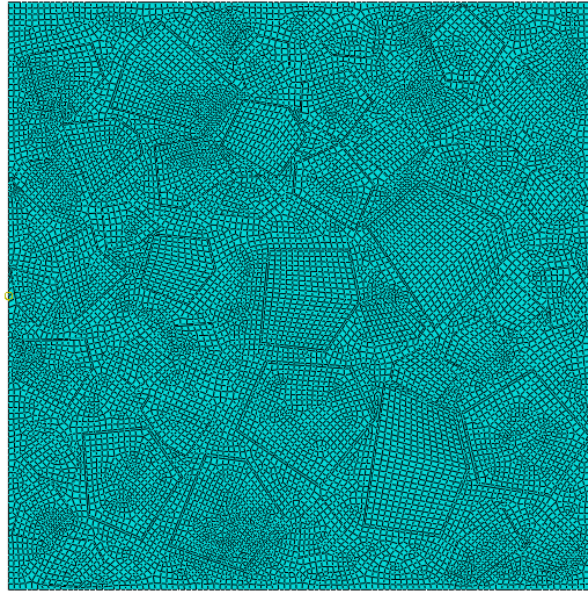
Where R_{θ} is the radius of the particle at a directional angle θ , and $R_{EE\theta}$ is the radius of an equivalent ellipse at a directional angle θ . Angularity index is a parameter independent

from aspect ratio or form ratio, it quantifies the morphology of aggregate particles at a different scale.

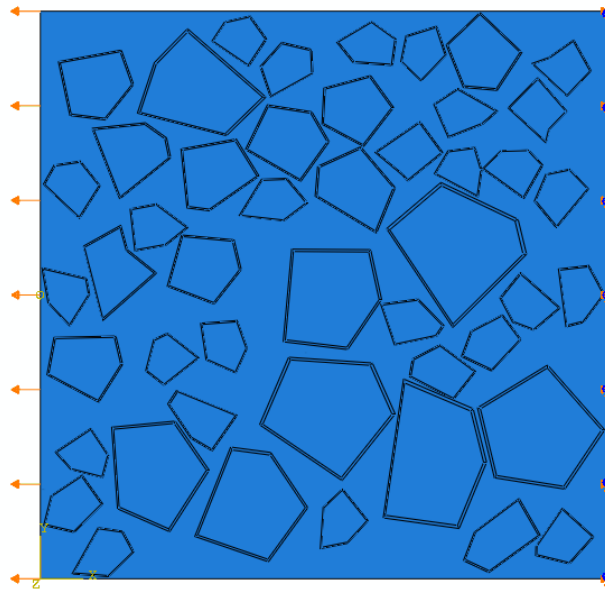
3.7 Analysis on Anisotropic Damage in Asphalt Concrete

Previous studies have investigated the stiffness anisotropy in asphalt concrete under undamaged conditions. It is necessary to understand the anisotropic behavior of asphalt concrete under the damaged condition. The developed model is able to take aggregate morphology into account in fracture analysis, which makes it possible to study the anisotropy of asphalt concrete under the damaged condition.

To study the anisotropy in the fracture behavior of asphalt concrete, the reference microstructure model was generated consisting of aggregates with aspect ratio of 1, angularity index of 14, and random orientation angles. The specimen was subjected to a 0.5mm tension displacement over one second at a constant strain rate. This strain is large enough to cause micro cracks within the material interface or FAM material, but not result in further crack propagation. The finite element model mesh and boundary conditions are plotted in Figure 3-15. Boundary conditions were changed to simulate asphalt concrete samples under tension in both vertical and horizontal directions.



(a)



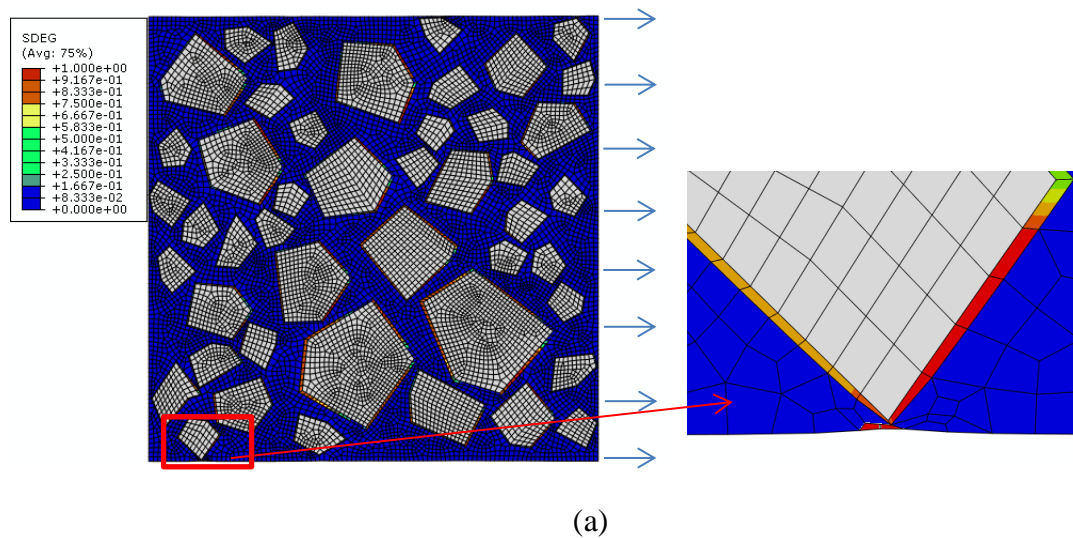
(b)

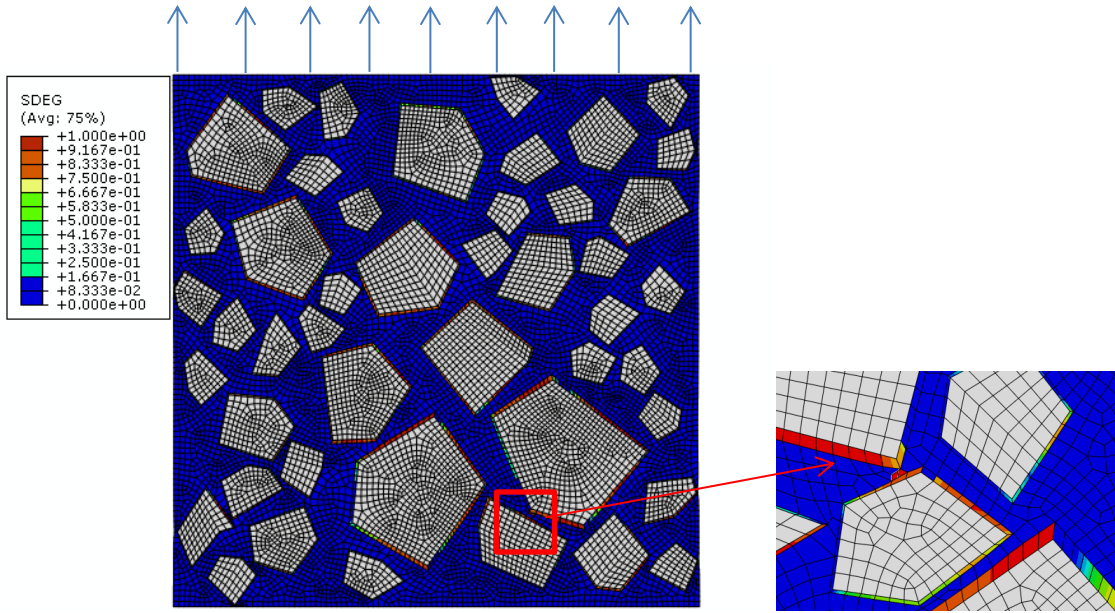
Figure 3-7 (a): The microstructure model mesh; (b) Load and boundary condition (horizontal tension).

The damage distributions in horizontal and vertical directions are shown in Figures 3-12 (a) and (b), respectively. It was found that micro cracks initiated in both horizontal and vertical loading conditions but they occurred at different locations within the asphalt

concrete sample. When tension was applied in the vertical direction, micro crack initiated within the FAM as the displacement reached 0.0125mm; when tension was applied in the horizontal direction, micro crack initiated in the FAM as the displacement reached 0.005mm. This indicates the initiation of cohesive crack is affected by the loading direction.

The average SDEG values of four elements closest to the micro crack were plotted in Figure 3-17. It shows that the interface damage (cohesive failure) induced by tension was greater when the load was applied in the horizontal direction compared to the damage induced by the loading in the vertical direction. In this case, even though the same displacement-controlled load was applied in horizontal and vertical directions, distinctive fracture behavior appeared. For the aggregate microstructure studied here, the loading in the horizontal direction resulted in earlier FAM fracture and higher level of interface damage. The damage anisotropy in asphalt concrete can be captured using the model proposed in this study.





(b)

Figure 3-16 Damage distributions when tension is applied in (a) horizontal and (b) vertical directions

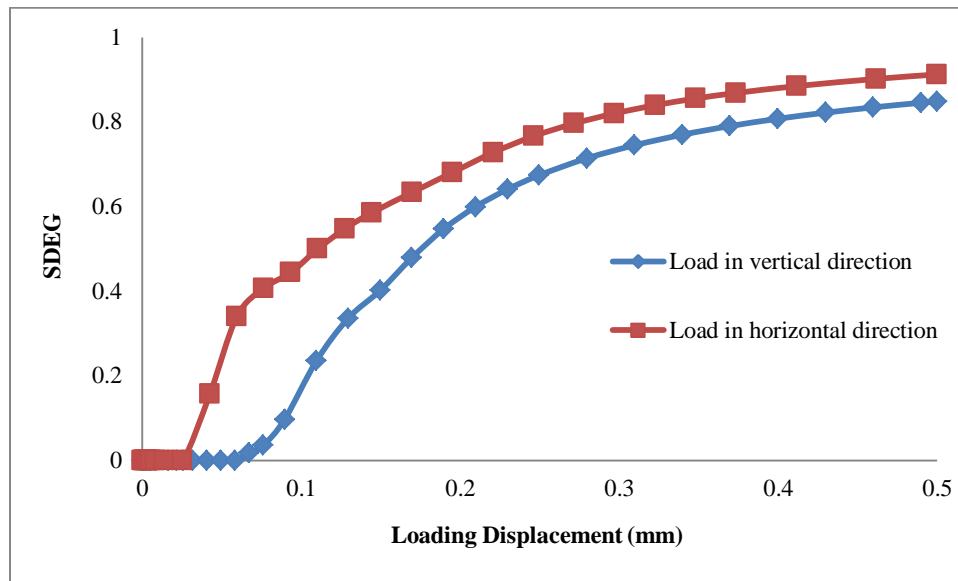


Figure 3-8 Interface damage near the crack within FAM

3.8 Parametric Study of Damage Anisotropy

3.8.1 Effect of Aggregate Angularity

It is expected that the sharpness of aggregates may affect the initiation of micro crack and performance of asphalt concrete. In this study, three angularity indexes were selected to generate the microstructure models in order to study the effect of aggregate angularity on the anisotropic damage behavior of asphalt concrete. The aggregate microstructures were generated with the AI values equal to 1, 7, and 15 with the same aspect ratio equal to one. The perfect circular aggregates have an angularity index of one and the aggregates become shaper as the value of AI increases. The detailed microstructures are shown in Figure 3-18. Each numerical model was subjected to the same amount of tension displacement in both horizontal and vertical directions.

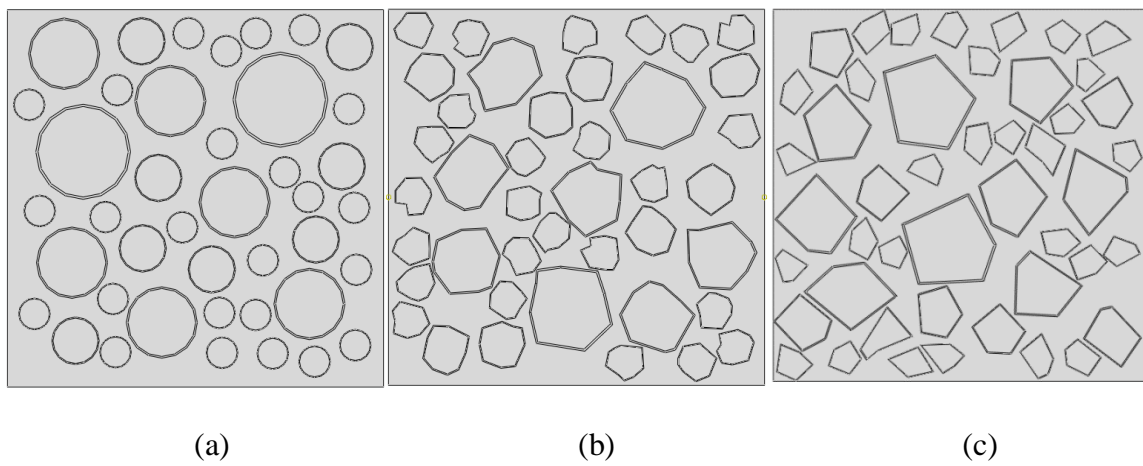


Figure 3-9 Microstructures of asphalt concrete samples with angularity index of (a) 1, (b) 7 and (c) 15.

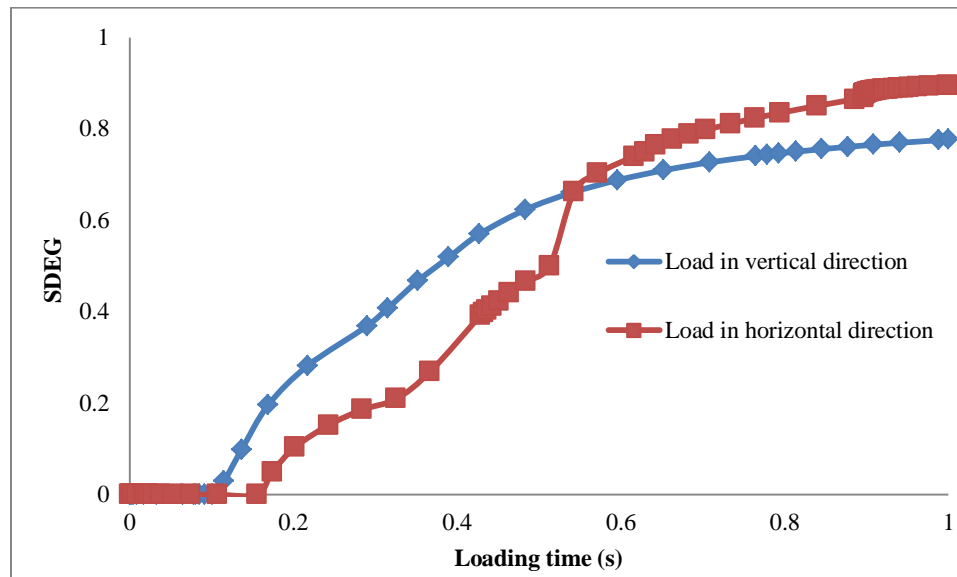
Table 3-4 shows the displacements required for the initiation of cohesive crack within the FAM of each sample when the tension is applied at different directions. Conclusions can be made that the more angular the aggregate is, the earlier the cohesive cracking would initiate within the FAM. The higher AI results in stress concentration near the sharp aggregate tip, which leads to cohesive fracture in the FAM. The displacements that are required for initiation of cohesive crack at two orthogonal

directions do not show a consistent trend regarding the effect of aggregate angularity on the initiation of cohesive damage.

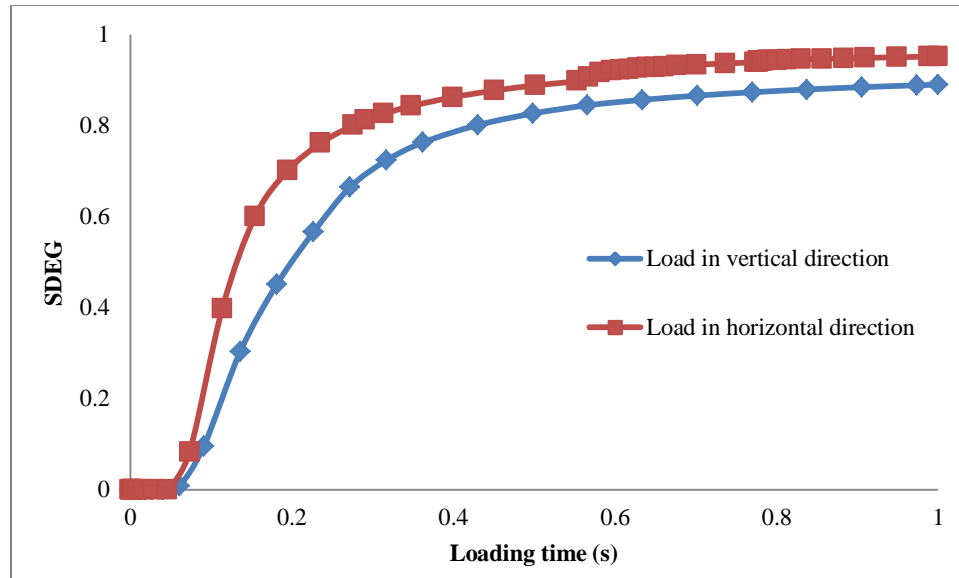
Table 3-4 Displacements required for crack initiation in FAM with different AIs

AI	Loading direction	Displacement required for initiation of cohesive crack (mm)
1	horizontal	0.015
	vertical	0.04
7	horizontal	0.008
	vertical	0.01
15	horizontal	0.006
	vertical	0.008

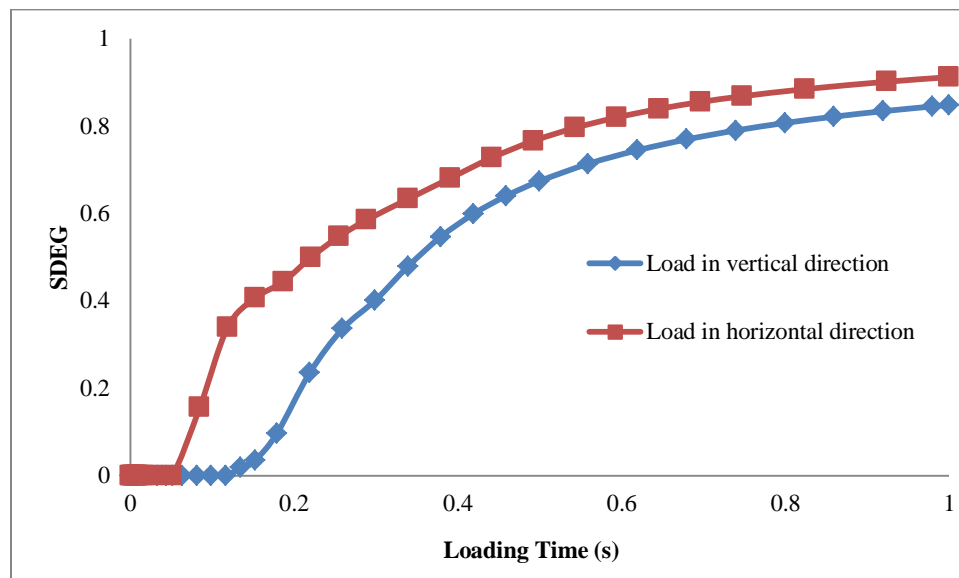
Figure 3-19 shows how the interface damage (average SDEG values) near the crack in the FAM evolved for each sample when the tension is applied at horizontal and vertical directions. All three samples show significant anisotropic damage behavior caused by tension. However, the level of anisotropy varies as the angularity index changes yet no obvious trend for the change was observed in this study.



(a)



(b)



(c)

Figure 3-10 Interface damage near the crack in FAM for samples with AI of (a) 1, (b) 7 and (c) 15.

3.8.2 Effect of Aspect Ratio and Orientation Angle

Asphalt concrete contains aggregates with different aspect ratios (or form ratios) that have direct influence on performance of asphalt concrete. When the aspect ratio is larger than one, orientation angle is needed to describe the spatial distribution of aggregates within asphalt concrete. It is difficult to quantitatively characterize the effect of orientation angle on performance of asphalt concrete with the traditional experimental method considering the challenge in preparing samples with a unified orientation angle. The microstructure generation method used in this study allows for accurate control of aspect ratio and orientation angle for each microstructure sample generated.

The coupled effects of aspect ratio and orientation angle were investigated. Two aspect ratios (one and two) and two orientation angles (0° and 45°) were considered in this study. As for aggregate with aspect ratio equal to one, the orientation angle does not pose significant influence on the spatial distribution of aggregate; only one model was generated as a reference case. The generated microstructure models are shown in Figure 3-20. All samples were subjected to tension at both horizontal and vertical directions with a loading rate of 0.5 mm/s.

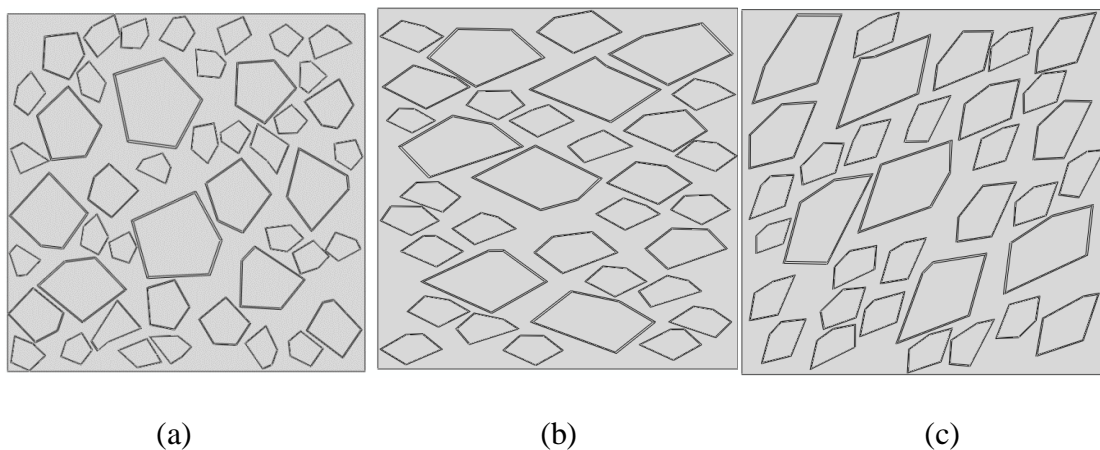


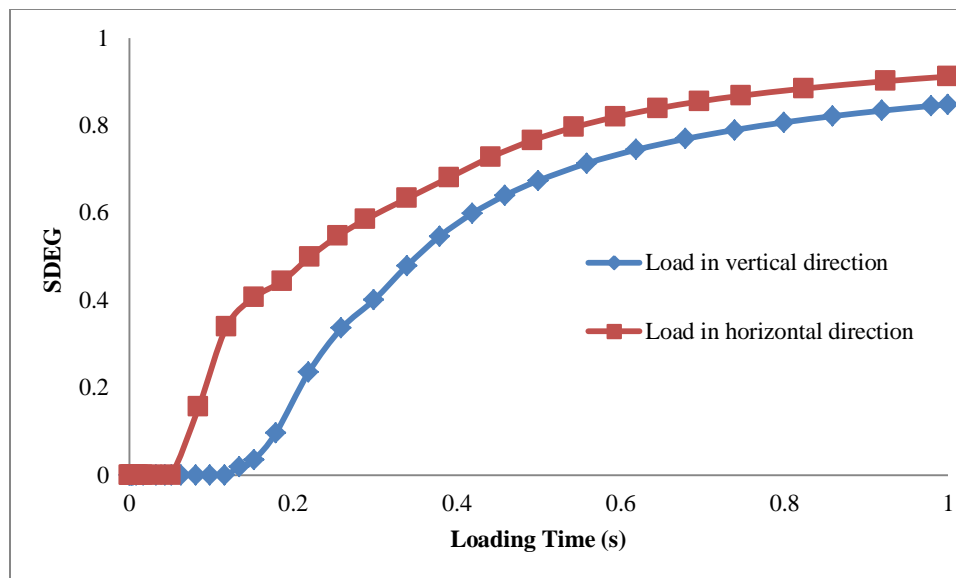
Figure 3-20 Microstructure of asphalt concrete with aggregate (a): aspect ratio of 1, (b) aspect ratio of 2, orientation angle 0° and (c) aspect ratio of 2, orientation angle 45° .

Table 3-5 compares the displacements required for initiation of cohesive crack in the FAM with different aspect ratios and orientation angles. Samples with uniform orientation angles showed more resistance for cohesive fracture, FAM fracture occurred earlier in the sample with random distributed aggregates.

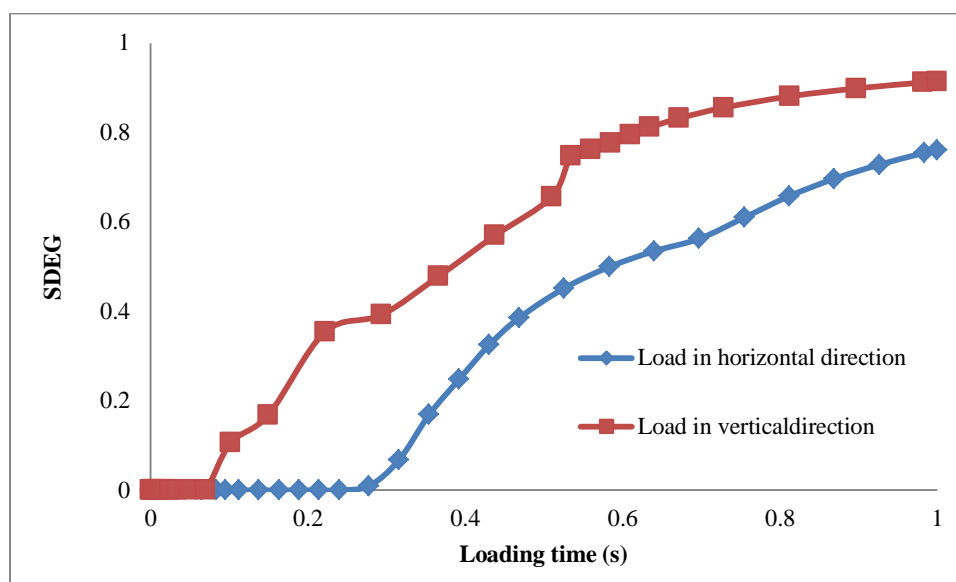
Table 3-5 Displacements required for crack initiation in FAM with different ARs and Orientation angles.

AR	Orientation Angle	Loading direction	Displacement required for initiation of cohesive crack (mm)
1	Random between 0-45	horizontal	0.006
		vertical	0.008
2	0	horizontal	0.01
		vertical	0.05
	45	horizontal	0.015
		vertical	0.075

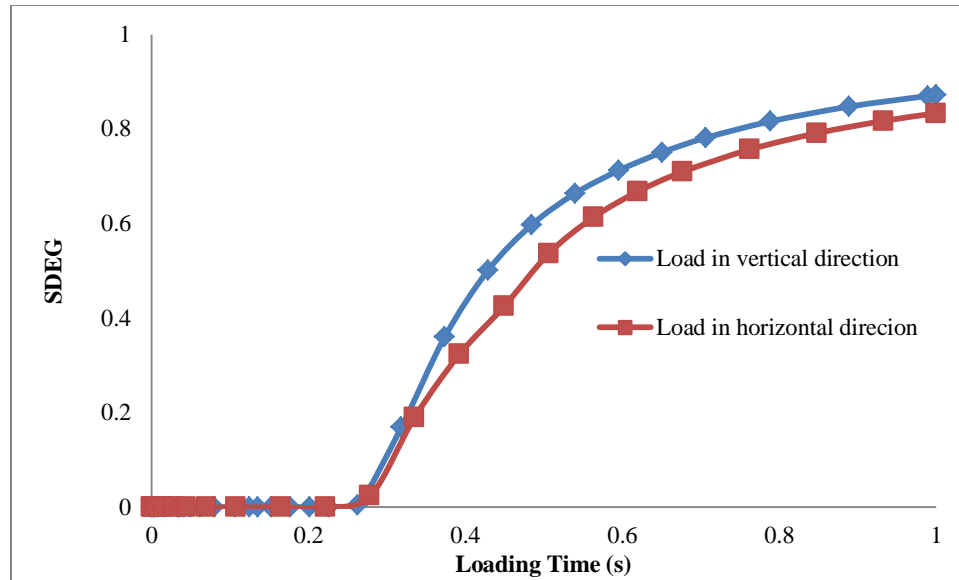
Figure 3-21 shows the SDEG values for elements near FAM cracks in different samples. Orientation angle played a key role in determining the damage anisotropy. For the sample with uniform orientation angle of 45°, the SDEG values near FAM crack showed similar developing trend when the sample was loaded in horizontal and vertical direction. As for the sample with a uniform orientation angle of 0°, the SDEG values showed a significant difference between vertical and horizontal direction. The sample with a uniform orientation angle of 45° has a near-isotropic geometry in horizontal and vertical directions while the sample with a uniform orientation angle of 0° shows the highest level of geometrical anisotropy. The damage anisotropy is linked directly with the aggregate shape and its spatial distribution.



(a)



(b)



(c)

Figure 3-21 Interface damage near the crack in FAM for samples with: (a) aspect ratio 1, (b) aspect ratio 2, orientation angle 0° and (c) aspect ratio 2, orientation angle 45° .

3.8.3 Effect of Maximum Aggregate Size

Aggregate size is another factor affects the fracture performance of asphalt concrete. Here three samples were generated with maximum aggregate size of 19 mm, 12.5 mm, and 9.5 mm. The microstructure of each sample is shown in Figure 3-22. Each sample was tested under tension in both vertical and horizontal directions with a loading rate of 0.5 mm/s to study the anisotropic effect.

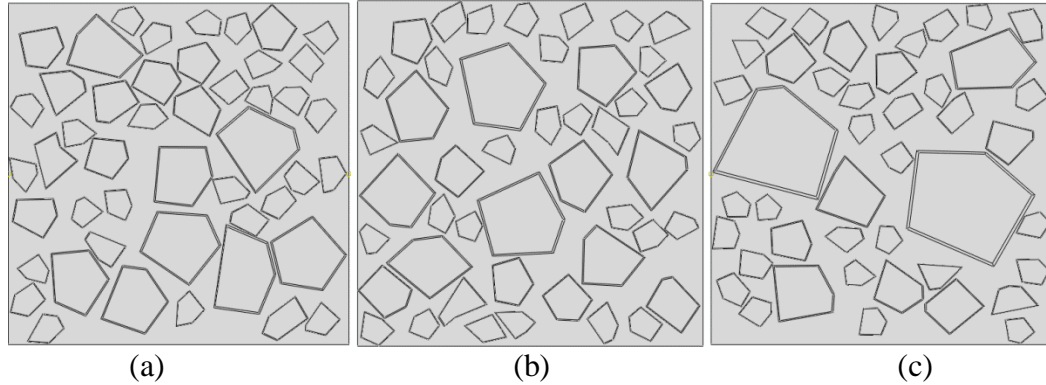


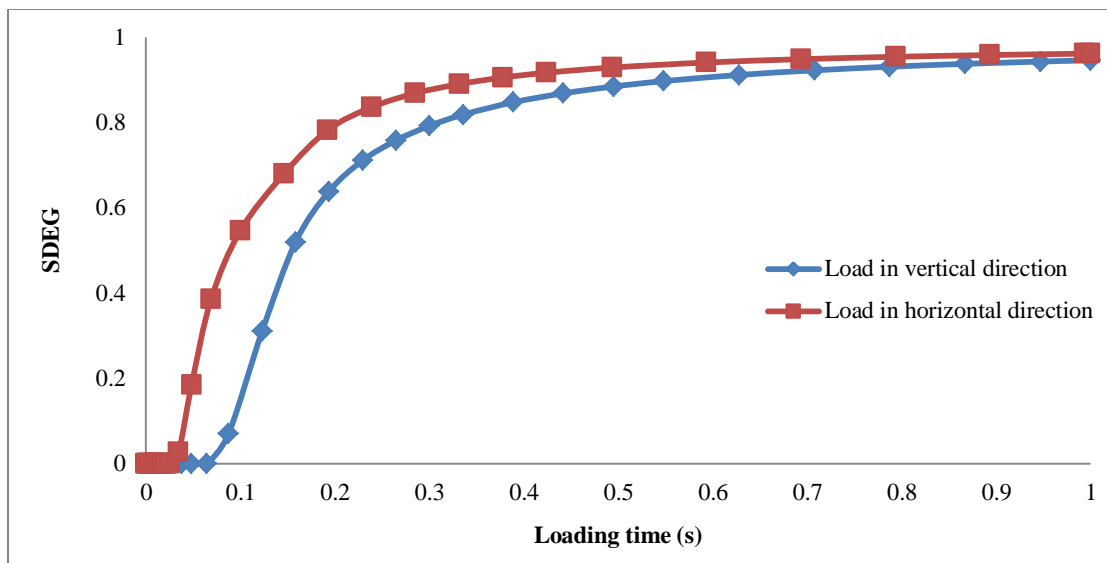
Figure 3-22 Microstructures of asphalt concrete with maximum aggregate size of (a) 9.5 mm, (b) 12.5mm and (c) 19 mm.

Table 3-5 compares the displacements required for initiation of cohesive crack in the FAM with different maximum aggregate sizes. The displacement required for crack initiation in FAM varies for samples with different maximum aggregate sizes. No apparent trend can be observed from the analysis result.

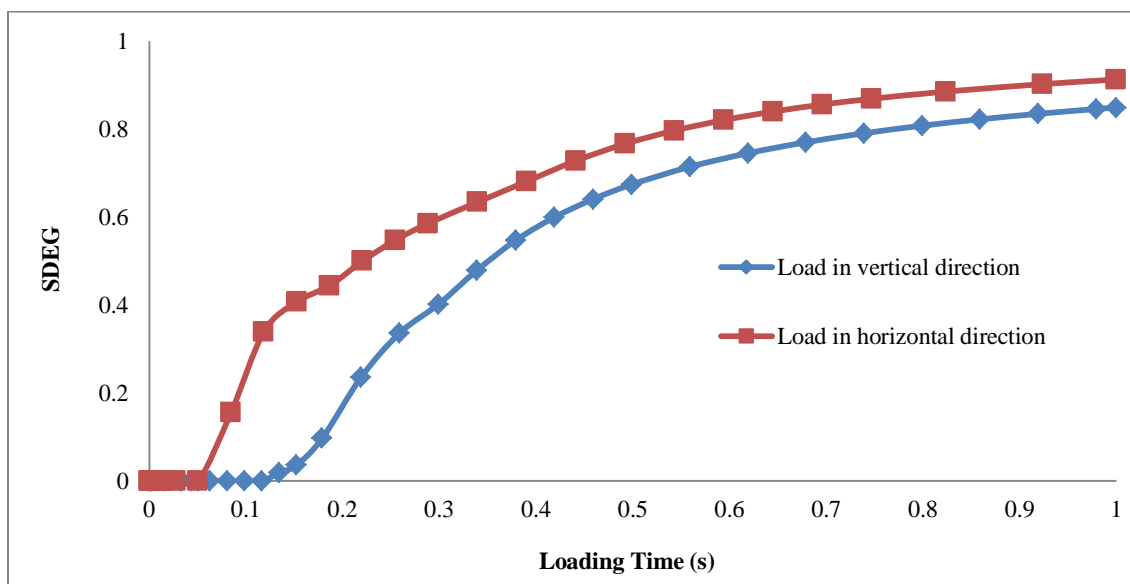
Table 3-6 Displacements required for crack initiation in FAM with different Maximum Aggregate Size

MAS	Loading direction	Displacement required for initiation of cohesive crack (mm)
19	horizontal	0.015
	vertical	0.01
12.5	horizontal	0.006
	vertical	0.008
9.5	horizontal	0.0025
	vertical	0.01

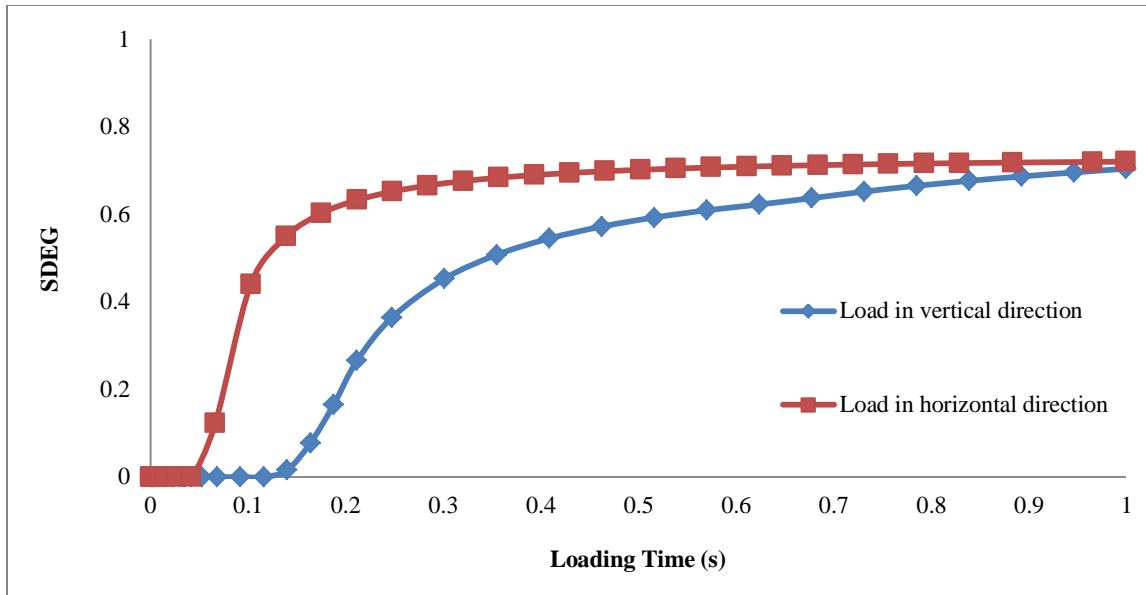
The differences in interface damage for the samples with different maximum aggregate sizes can be seen in Figure 3-21. The samples with maximum aggregate size of 19mm show the highest level of interface damage. As the maximum aggregate size drops, the damage level decreases. Large aggregate size results in higher interface damage under tension load if the total aggregate content is kept the same.



(a)



(b)



(c)

Figure 3-21 Interface damage near the crack in FAM for samples with: (a) maximum aggregate size of (a) 19mm, (b) 12.5mm and (c) 9 mm.

3.9 Summary

A micromechanical analysis model was developed in this study to analyze the fracture behavior of heterogeneous asphalt mixtures. The extended finite element method and cohesive zone elements were incorporated together with randomly generated microstructures to simulate the cohesive and adhesive fracture behaviors of asphalt mixtures, respectively. Asphalt mixture samples under tension loading conditions were simulated and the sensitivity of fracture resistance to different material and fracture parameters was studied. Meanwhile, emphasis was focused on the influence of aggregate angularity, aspect ratio, orientation angle, and size effect on the fracture performance. Each microstructure model was subjected to tension load in both horizontal and vertical directions to study the anisotropy of asphalt concrete performance.

The numerical analysis of the microstructure model indicates that the development of cracking shows that the damage in the FAM material would initiate first at a small displacement and then interconnect with the damage developed at the FAM-aggregate interface; the critical locations for crack initiation in the FAM material were found in the area where an aggregate tip is close to the boundary of another aggregate or where an aggregate tip is close to the sample boundary and the higher FAM modulus due to low temperatures or high loading rates could result in the greater fracture potential in asphalt mixtures. As for the influence of aggregate morphology on damage anisotropy: Aggregates with higher angularity index induced higher damage under tension. The anisotropic damage effect was significantly influenced by the aspect ratio and orientation angle. This indicates that the damage anisotropy is closely associated with aggregate shape and spatial distribution anisotropy. Larger aggregates in size resulted in higher damage within asphalt concrete.

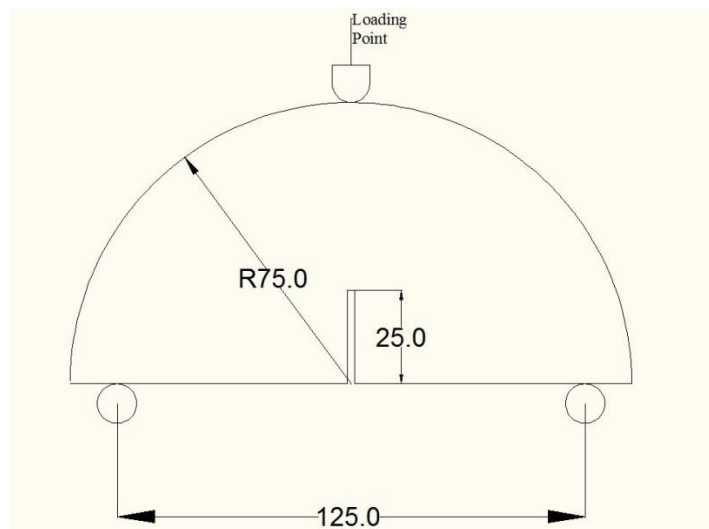
CHAPTER 4. FRACTURE SIMULATION OF ASPHALT CONCRETE IN SEMI-CIRCULAR BENDING TEST

4.1 Finite Element Model of SCB Test

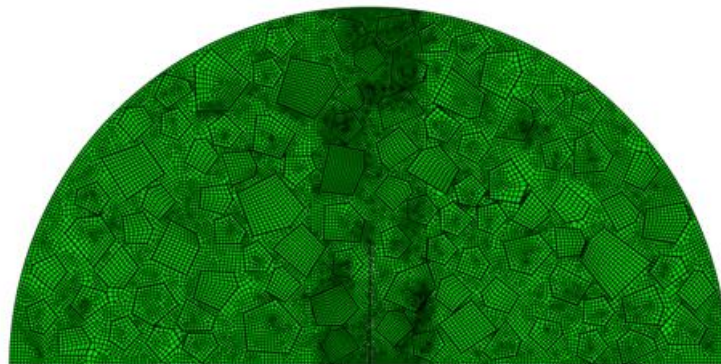
To understand the fracture behavior of asphalt concrete, different experimental test setups have been proposed by researchers, including the single-edge notched beam (SEB) test (*Mobasher et al., 1997; Hoare et al., 2000; Marasteanu et al., 2002; and Wagoner et al., 2005*), the disc-shaped compact tension (DCT) test (*Lee et al., 1995; Wagoner et al., 2005, 2006*), the double-edged notched tension (DENT) test (*Seo, 2003*), and the semi-circular bending (SCB) test (*Molenaar et. al. 2002; Li and Marasteanu 2004 and 2006*). The specimen geometry of the tested samples and the stress states generated in the testing vary among these tests. The fracture energy and strength are usually two most important fracture properties obtained from the fracture test for characterizing the global fracture behavior of asphalt concrete. Despite the limitations of relatively small fracture area, SCB test setup is more popular than other test setups for several reasons. For example, the test is repeatable and easy to perform with test samples that can be prepared from Superpave gyratory specimen or field cores. Another advantage is the dimension of the sample being smaller compared to SEB, DENT, and DCT.

The standard SCB test sample is semi-circle shaped with two supporting points at the bottom and one loading point on the top. The sample is 150 mm in diameter with a 25-mm notch in the middle. The supporting points are located 12.5 mm away from the edge in the bottom. In the real testing environment, a loading line displacement (LLD)

gauge is attached to the sample to measure the sample displacement. Along with LLD gauge also a crack mouth opening displacement (CMOD) gauge is set near both sides of the notch. The finite element model was developed using the commercial software ABAQUS version 6.10 (23). Figure 4-1(a) shows the SCB standard setup. The initial notch was modeled as an initial crack. The boundary conditions were set as fixed on one side and simple support on the other side with displacement controlled loading applied on top of the sample. The element size was selected from sensitivity analysis based on the principle that the increase of element size will not affect the crack propagation path.



(a)



(b)

Figure 4-1 (a) Standard SCB Test Setup, and (b) finite element model of randomly generated microstructure of asphalt concrete

4.2 Model Validation with Experimental Results

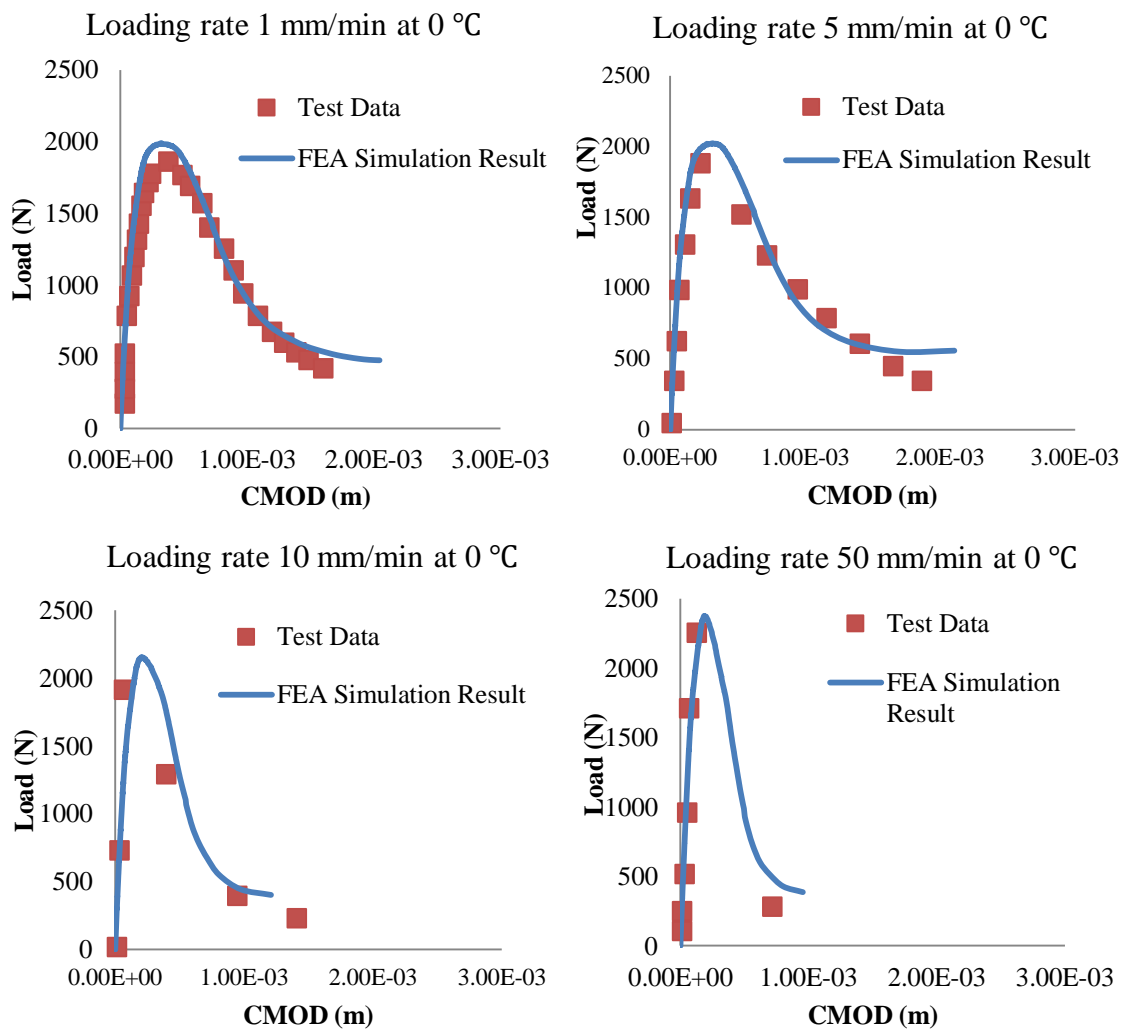
In an earlier study by Im (2012), asphalt concretes were tested using the SCB setup under different loading rates and temperatures. A cohesive zone model (CZM) based finite element analysis was carried out to obtain the homogeneous fracture properties of asphalt concretes by compared to the test data. In this study, a heterogeneous model with XFEM was developed for simulating the SCB test, as shown in Figure 4-1 (b). The asphalt concrete consists of two main phases: coarse aggregate and FAM. The FAM is defined as a combination of asphalt binder and fine aggregate (passing sieve size 2.36 mm). The two main phases have different mechanical properties and it is necessary to model them separately. The aggregate normally has high elastic modulus and fracture strength and behaves as a linear elastic material. Meanwhile the asphalt binder is highly viscoelastic and has lower modulus and fracture strength compared to the aggregate. The aggregate gradation that was used to generate the microstructure of asphalt concrete and the viscoelastic parameters of FAM are listed in Table 4-1 (Im, 2012). The Poisson's ratios were assumed to be 0.3 for FAM and 0.15 for coarse aggregates.

TABLE 4-1 Aggregate Gradation and Linear Viscoelastic Properties of FAM (Im, 2012)

E=50GPa	Sieve Size (mm)	Passing Percentage (%)	Reference Temperature	21 °C	E ₀ =17.6GPa	
Coarse Aggregate	19	100	Prony Series Parameters of FAM	E _i (MPa)	ρ _i (sec)	
	12.5	95		1	9010.5	2E-5
	9.5	89		2	8776.6	2E-4

	4.75	72	3	4062.5	2E-3
FAM	2.38	36	4	2347.2	2E-2
	1.19	21	5	927.8	2E-1
	0.6	14	6	455.7	2E+0
	0.3	10	7	183.8	2E+1
	0.15	7	8	95.1	2E+2
	0.075	3.5	9	43.6	2E+3

The simulations were conducted at the same loading rates and temperatures as used in the experimental tests (*Im 2012*): loading rate of 1 mm/min, 5 mm/min, 10 mm/min, and 50 mm/min at 0°C and -10°C. These two temperatures were selected in the simulation considering that fracture is the major failure mechanism of asphalt concrete at low temperatures. The simulation results were compared to the experimental data, as shown in Figure 4-2. The fracture behavior of asphalt concrete varies at different temperatures and loading rates due to viscoelasticity of asphalt binder. The fracture behavior of asphalt concrete varies at different temperatures and loading rates due to viscoelasticity of asphalt binder. The viscoelastic material model of FAM successfully characterizes how the fracture behavior changes at different temperatures and loading rates.



(a)

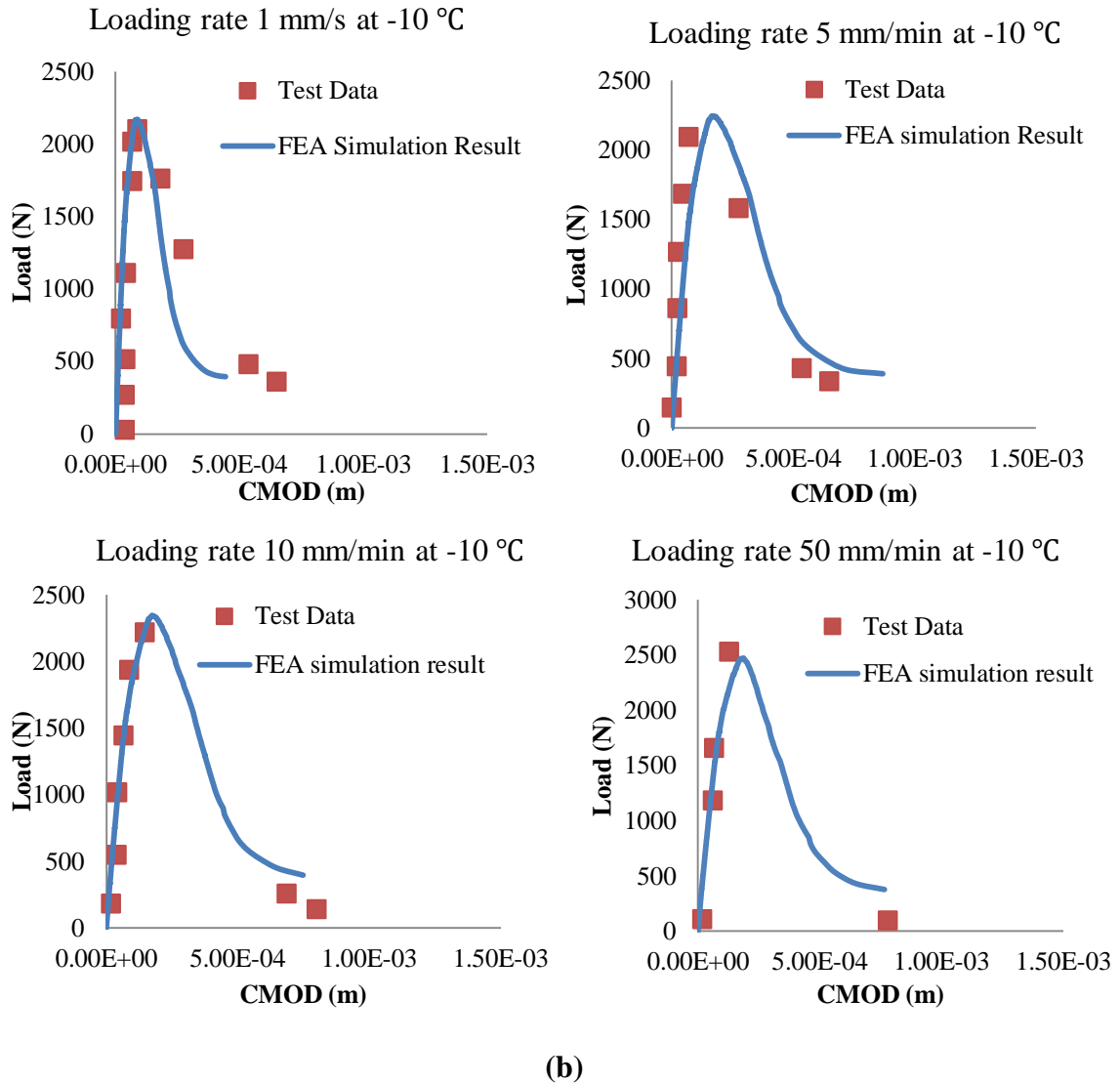
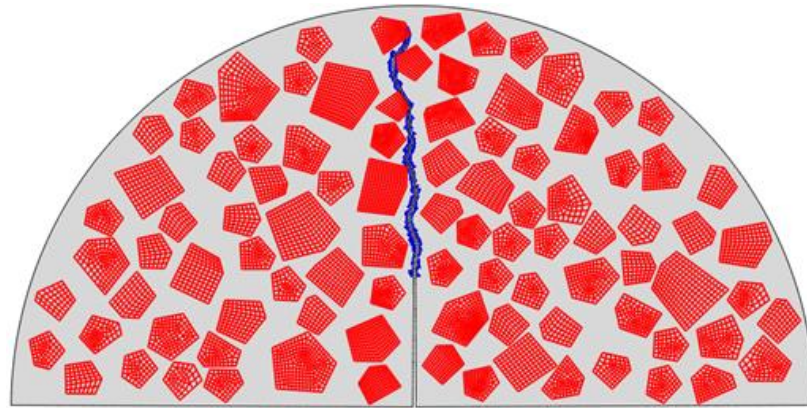


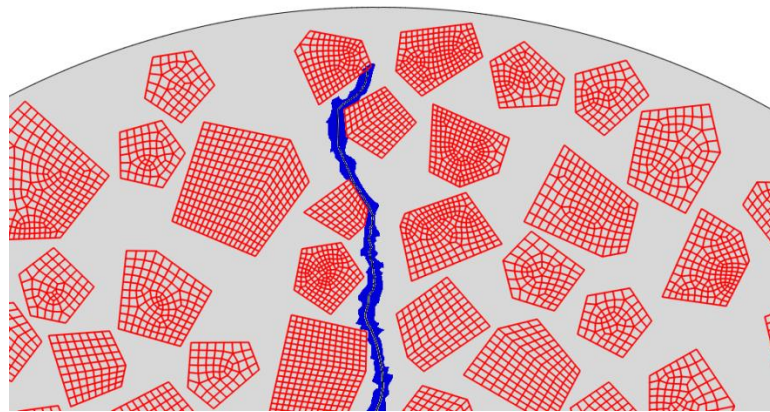
Figure 4-2 Fracture simulation results at (a) 0°C and (b) -10°C as compared to testing data reported by Im (2012)

The heterogeneous model proposed in this study provides simulation results for both crack propagation path and the overall fracture behavior. The crack path within the asphalt concrete is shown in Figure 4-3. The observation of crack path shows that crack happens mostly within the FAM material. The crack would go around the coarse aggregate when the crack path was approaching an aggregate. This crack pattern agrees

with observations from previous experimental tests and numerical simulations (Wagoner et al. 2005, Y.R. Kim et al. 2007). It indicates that the fracture properties of the FAM material played a key role in affecting the overall fracture behavior.



(a)



(b)

Figure 4-3 (a) Crack propagation path and (b) localized zoom-in near the crack tip

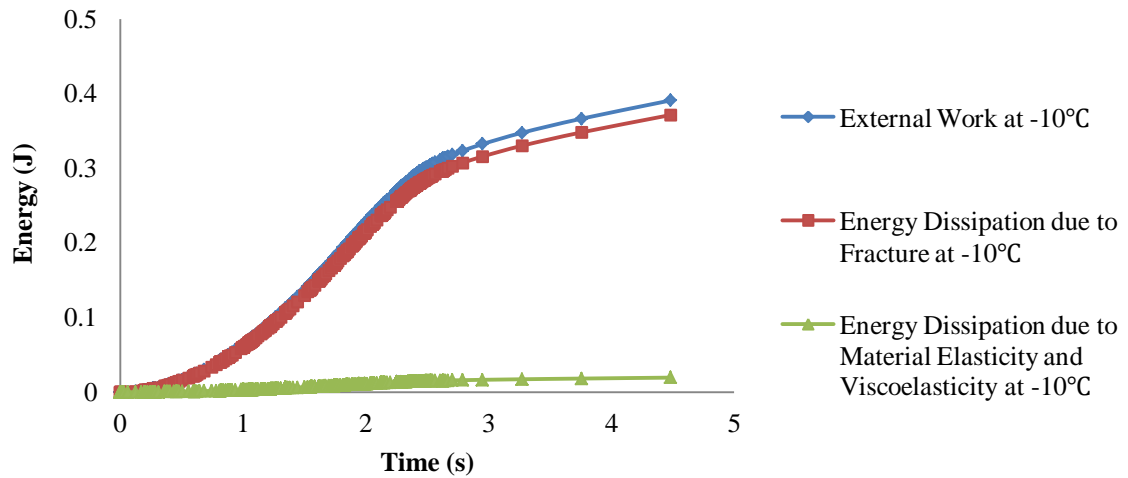
4.3 Parametric Study

4.3.1 Effect of Temperature and Loading Rate

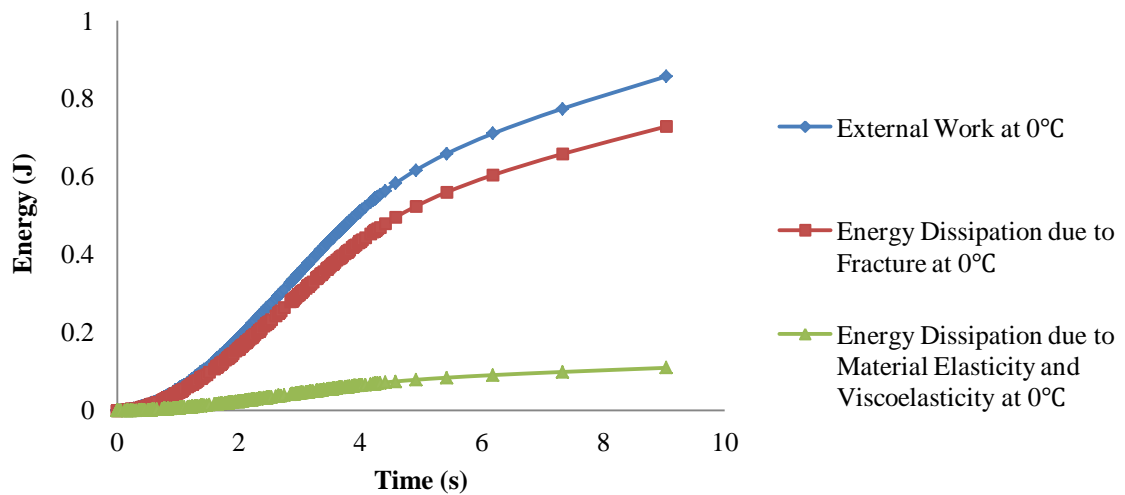
The asphalt concrete becomes brittle at low temperatures because the fracture properties change significantly when the temperature varies. A lower temperature results in a higher modulus due to the viscoelastic characteristics of asphalt binder and it leads to a higher

peak load. Evaluation of energy dissipation was conducted using the simulation results. The energy dissipation components of the sample under 5-mm/min loading rate at -10°C and 0°C are shown in Figure 4-4. The fracture energy at 0°C is higher than the fracture energy at -10°C . The asphalt concrete shows linear elastic characteristics at -10°C . At -10°C , most of the external work dissipated through fracture; only 5% of the energy dissipated through material viscoelasticity. The viscoelastic behavior becomes obvious when the temperature increases to 0°C . At 0°C , 15% of the total external work dissipated due to material viscoelasticity. Temperature is a vital factor in evaluating the fracture performance of the asphalt concrete. The energy dissipation analysis explains why the pavements are prone to crack at lower temperatures.

The loading rate significantly affects the elastic modulus and fracture properties of the FAM material viscoelasticity. Figure 4-5 shows how the loading rate affects the fracture properties obtained from the simulation results. It shows that the peak load increases as the loading rate increases at both temperatures. However, the fracture energy does not change when the sample is subjected to different loading rates at -10°C , but the fracture energy drops as the loading rates increases at 0°C . The asphalt concrete shows elastic characteristics at relatively lower temperature, -10°C here. The loading rate affects the asphalt concrete in a different way when the sample is subjected to different temperatures.

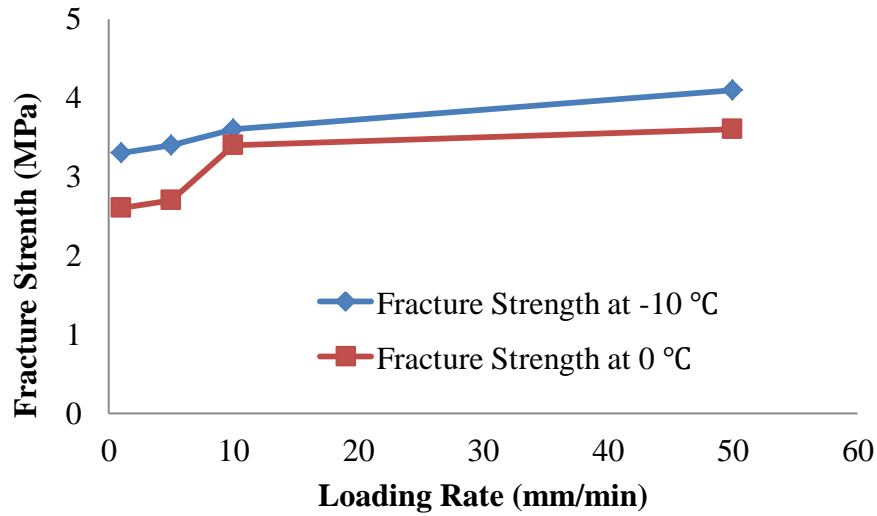


(a)

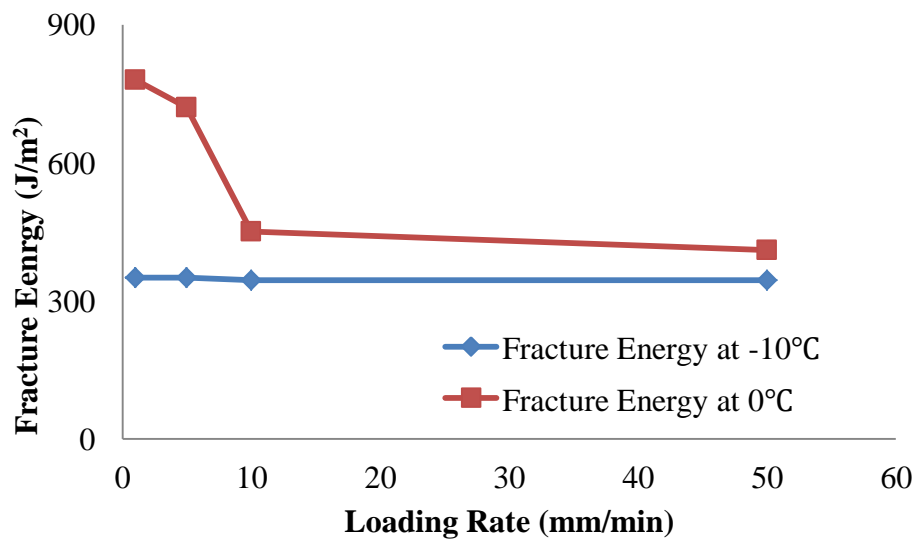


(b)

Figure 4-4 Energy Dissipation Condition at (a) 0°C and (b) -10°C



(a)



(b)

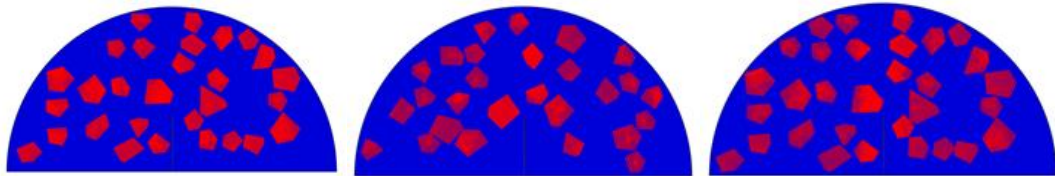
Figure 4-5 Effect of loading rate on (a) fracture strength and (b) fracture energy

4.3.2 Effect of Aggregate Spatial Distribution

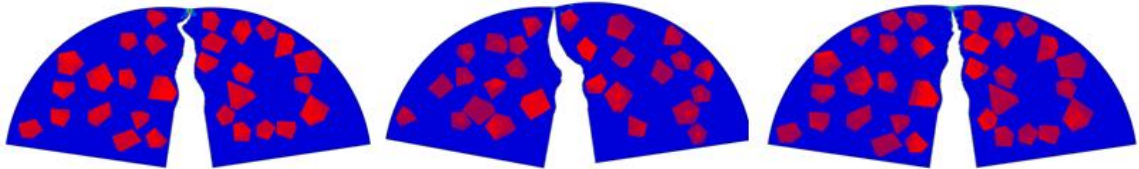
The aggregate microstructure was generated with the aggregate sizes over 4.75 mm to study the effect of coarse aggregate on fracture behavior of asphalt concrete, including aggregate spatial distribution, angularity, and gradation/size. The samples were generated

and simulated subject to 5-mm/min loading rate at 0 °C. The fracture strength and fracture energy of FAM material were set as 3.6 MPa and 700 J/m².

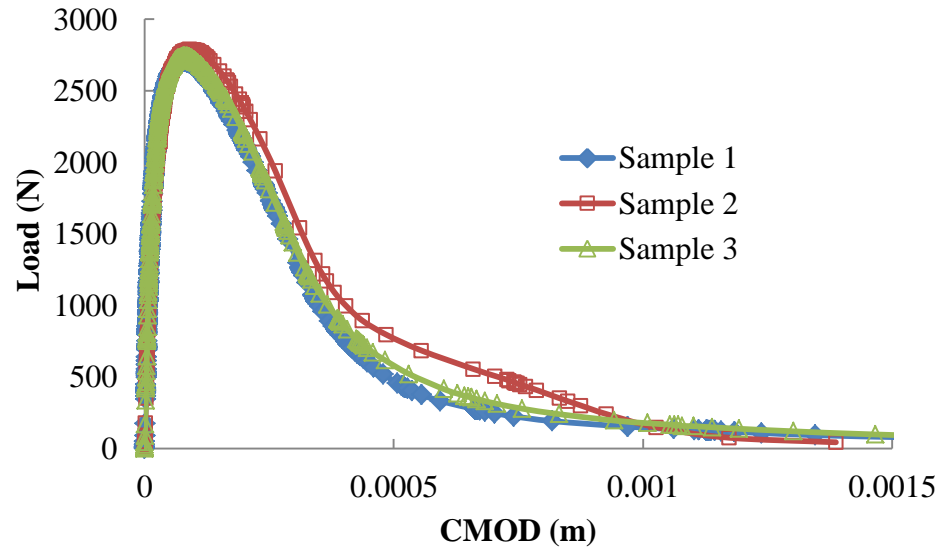
Three different samples were generated according to the same gradation to analyze the effect of coarse aggregate spatial distribution. Figures 4-6 (a), (b) and (c) shows the aggregate microstructure, crack paths, and fracture response curves of three samples, respectively. The aggregate shape characteristics were controlled with the aspect ratio close to one and the average angularity index equal to 15. The results show that the crack path is sensitive to the coarse aggregate distribution; while the response curves of three samples show that the overall fracture resistance is not sensitive to the coarse aggregate spatial distribution.



(a)



(b)



(c)

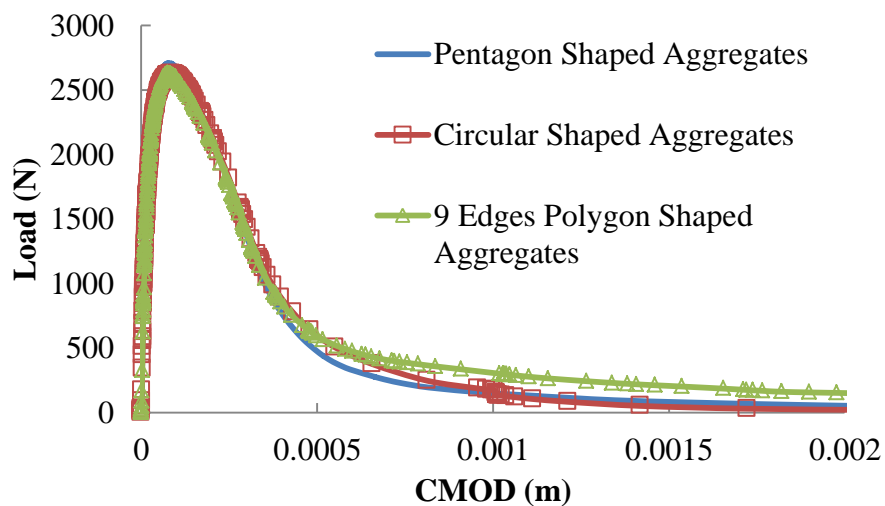
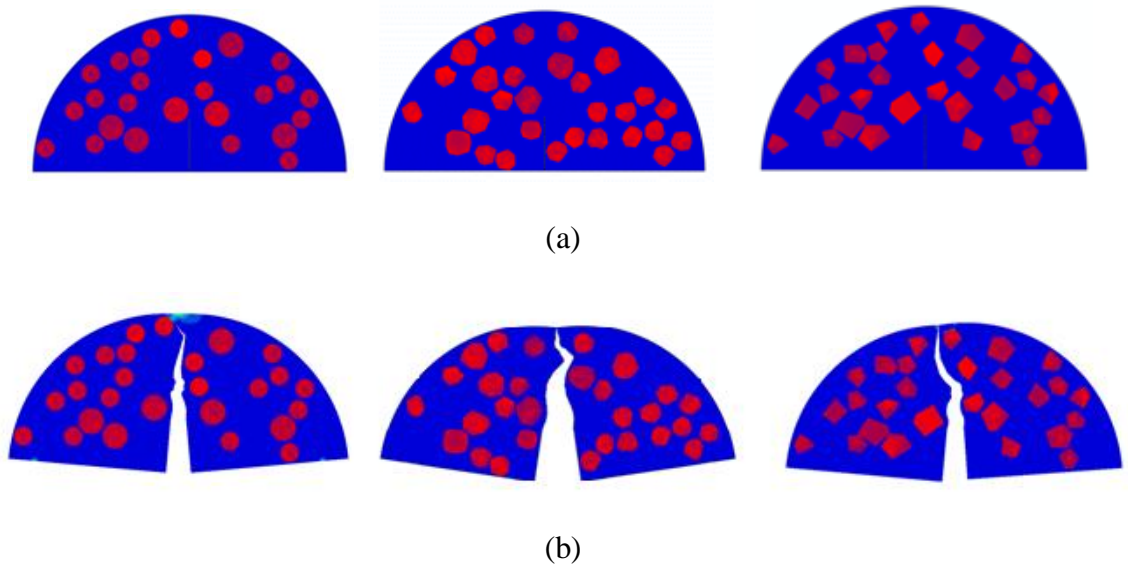
Figure 4-6 (a) Random microstructures, (b) crack paths, and (c) load-CMOD curves for SCB specimen with different spatial distributions

4.3.3 Effect of Aggregate Angularity

Different aggregate microstructures were generated with circular, pentagon, 9-edge polygon shaped aggregates to analyze the effect of aggregate angularity on fracture behavior. The aspect ratio of aggregate was controlled close to one; while the angularity index of aggregate is equal to 1, 7, and 15 for the circular, 9-edge polygon, and pentagon shaped aggregate, respectively. Figures 4-7 (a), (b) and (c) shows the aggregate microstructure, crack paths, and fracture response curves of three samples, respectively.

The angular aggregate could cause a non-uniform stress distribution around the coarse aggregate that could result in mixed-mode crack propagation. It was found that the crack path changed as the coarse aggregate angularity varied, yet the overall fracture responses were similar. This indicates that the coarse aggregate angularity may affect the initiation and development of localized damage in the asphalt concrete but have a weak

effect on the global fracture behavior. Previous studies have reported that the shape of coarse aggregates had little effect on the ultimate tensile strength of concrete but the crack propagation paths were under the influence of aggregate shapes (Ng *et al.* 2011, S.M. Kim *et al.* 2011). The simulation results here confirmed their findings from both local and global fracture behavior. It is noted that the coarse aggregate-FAM interface effect was not considered in the current model, which is one of the limitations of this study. Further investigation and supporting test results are needed to fully verify this finding.

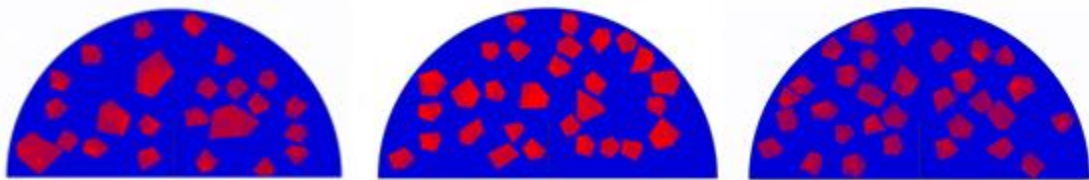


(c)

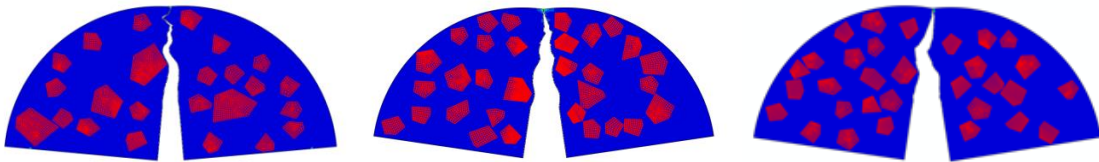
Figure 4-7 (a) Aggregate distributions, (b) crack propagation paths, and (c) load-CMOD curves for SCB specimen with different aggregate AI values

4.3.4 Effect of Aggregate Gradation and Size

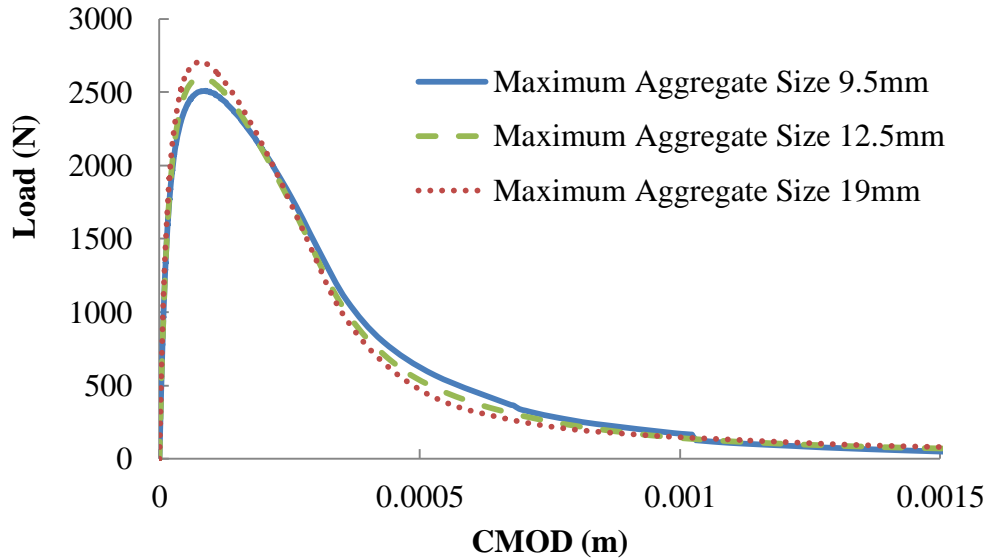
The effect of gradation and size of coarse aggregate on fracture behavior of asphalt concrete was investigated by changing the maximum aggregate size and gradation under the same mass (volume) fraction of aggregate. Three maximum aggregate sizes (19 mm, 12.5 mm and 9.5 mm) were used in the generation of aggregate microstructure with the aspect ratio close to one and the average angularity index equal to 15. Figures 4-8 (a), (b) and (c) shows the aggregate microstructure, crack paths, and fracture response curves of three samples, respectively.



(a)



(b)



(c)

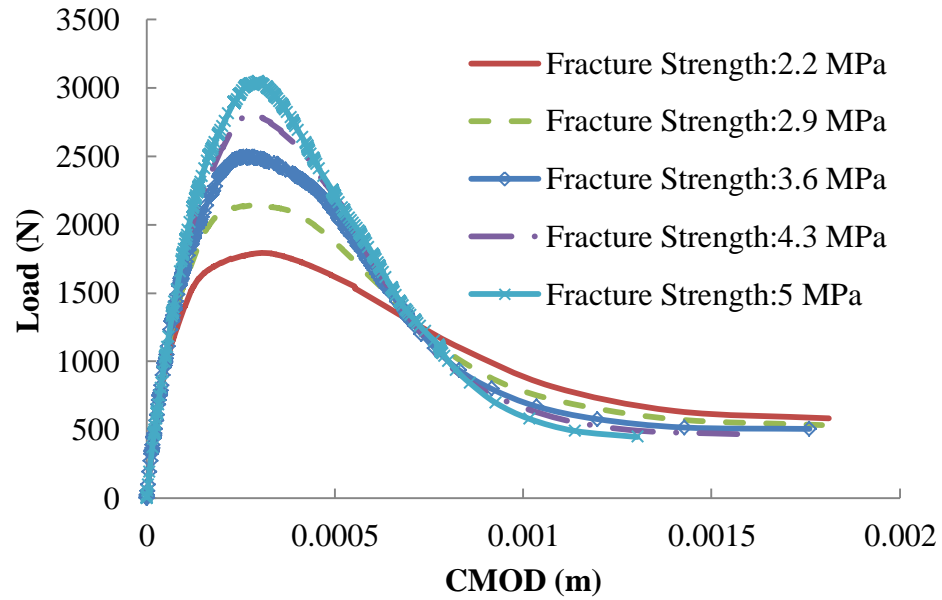
Figure 4-8 (a) Random microstructures, (b) crack paths, and (c) load-CMOD curves for SCB specimen with different aggregate gradations and sizes

It was found that the fracture strength and accordingly fracture energy increase as the maximum aggregate size increases with the same total aggregate content. As the aggregate size increases with the same aggregate content, the aggregate particles are fewer and the aggregate boundary area decreases. This may reduce the local stress concentration area around the aggregate and increase the total fracture resistance. This indicates that the gradation and size of coarse aggregate has more significant effect on fracture behavior of asphalt concrete as compared to the aggregate angularity. In real practice, as the aggregate gradation changes, the FAM properties may also change due to the change of binder content and air void in the mix design. This makes it difficult to study the effect of aggregation effect on fracture behavior of asphalt concrete using experimental results.

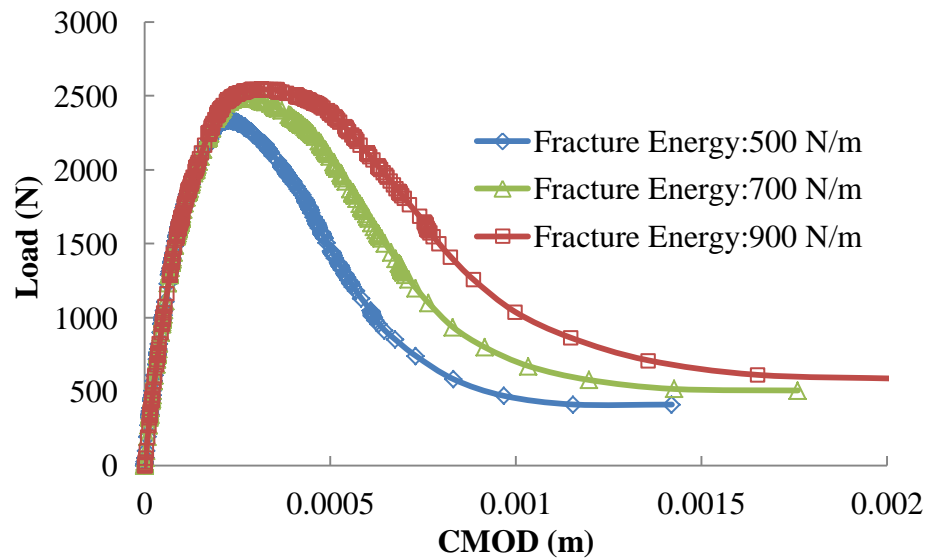
4.3.5 Effect of Fracture Parameters of FAM

The fracture strength and fracture energy of FAM are two governing factors in modeling the fracture process because they together control when crack would initiate and the energy to propagate forward. Figure 4-9(a) shows how the load-CMOD curve changes as the fracture strength of FAM changes from 2.2 MPa to 5 MPa. The peak load increases as the fracture strength increases. Higher fracture strength guarantees that the asphalt concrete would provide enough stiffness before it degrades due to fracture. The sensitivity analysis for fracture energy of FAM is shown in Figure 4-9(b). The peak load increases as the fracture energy increases but not by a large amount. Therefore, the peak load is not as sensitive to fracture energy as to fracture strength of FAM. Although increasing fracture energy of FAM may not improve the peak load, it reduces the crack propagation rate after peak load. High fracture energy would slow down the fracture process even a crack has already initiated within the asphalt concrete.

The results in this study offer insights on material design to have better fracture resistance of asphalt concrete. If the design focus is on providing high stiffness to support large and heavy vehicles, asphalt concretes with high fracture strength should be used in construction. If the focus is to design a pavement where cracking is inevitable and happen gradually, mixtures with high fracture energy should be considered to prevent the cracking and increase the durability.



(a)



(b)

Figure 4-9 Sensitivity analysis results for (a) fracture strength and (b) fracture energy of FAM

4.4 Summary

This chapter investigated the fracture behavior of asphalt concrete with randomly generated heterogeneous microstructure. The heterogeneous model with viscoelastic behavior was successful in simulating fracture behavior of asphalt concrete at different temperatures and loading rates. The distribution and angularity of coarse aggregate have an influence on crack path; but the overall fracture resistance does not change much when asphalt concrete samples are prepared using the same aggregate gradation. Increasing fracture strength and fracture energy of the FAM material significantly improves fracture resistance of asphalt concrete. The results indicate that the fracture behavior of asphalt concrete can be effectively predicted with viscoelastic and fracture parameters of FAM material and coarse aggregate gradation. Improvement is needed in future research to take into consideration the effect of aggregate-FAM interaction and air voids on fracture resistance of asphalt concrete.

CHAPTER 5. CONCLUSIONS AND FUTURE WORK

This thesis focuses on studying fracture behavior of asphalt concrete with a numerical analysis approach. Finite element models were built with the capacity of taking heterogeneity into consideration; asphalt concrete was modeled as heterogeneous material with coarse aggregates and fine aggregate matrix (FAM). Viscoelastic properties were assigned to the FAM. Different damage models were incorporated to study fracture at two length scales: micro fracture within FAM and coarse aggregate-FAM interface and global fracture resistance in the semi-circular bending (SCB) test. For micro fracture simulation, asphalt mixture was modeled as a multi-phase heterogeneous material with both adhesive and cohesive failure potential. Two different fracture models, cohesive zone model (CZM) and extended finite element model (XFEM), were adopted to simulate the fracture damage within the FAM (cohesive failure) and at the FAM-aggregate interface (adhesive failure), respectively. For global fracture behavior, the SCB test was simulated to evaluate crack propagation pattern and load-crack mouth opening displacement (CMOD) curve of asphalt concrete. Parametric studies with different material properties of FAM and coarse aggregates-FAM interface, morphological characteristics of coarse aggregates, and testing conditions (loading rate and temperature) were carried out to study their effects on the fracture behavior of asphalt concrete.

5.1 Findings on Micromechanical Analysis of Asphalt Mixture Fracture

1. The development of cracking shows that the damage in the FAM material would initiate first at a small displacement and then interconnect with the damage developed at the FAM-aggregate interface. As the displacement keeps increasing, the interface adhesive damage becomes the dominant failure mode.

2. The critical locations for crack initiation in the FAM material were found in the area where an aggregate tip is close to the boundary of another aggregate or where an aggregate tip is close to the sample boundary. This indicates that high aggregate angularity may cause premature fracture failure although it provides skeleton structure to prevent shear-induced rutting.
3. Although the critical failure locations may vary depending on the microstructure of asphalt mixture, the global failure potential at the specimen level does not vary significantly with the randomly generated aggregate microstructure using the same aggregate gradation.
4. The higher FAM modulus due to low temperatures or high loading rates could result in the greater fracture potential in asphalt mixtures. Better interface bonding strength between the aggregate and binder could significantly improve the fracture resistance of asphalt mixtures. Aged asphalt concrete are severely prone to fracture in the interface between FAM and coarse aggregates.

5.2 Findings on Microstructure-Induced Anisotropy in Damaged Asphalt Concrete

1. The anisotropic damage behavior was simulated using the heterogeneous interface model proposed in this study. Different crack initiation locations and timings were observed in the simulation results when the sample was loaded in two orthogonal directions. The damage pattern and damage level were different in vertical and horizontal directions.
2. Aggregates with high angularity index results in higher damage level within asphalt concrete. The asphalt concrete sample with circular aggregates (AI=1) showed highest resistance to fracture in the FAM and FAM-aggregate interface.

The sharp aggregates are not ideal for facture-resistant design in asphalt concrete even though they are normally considered to perform better when it comes to rutting.

3. Damage anisotropy links directly with the aggregate shape and spatial distribution. When the asphalt concrete sample shows more apparent microstructural anisotropy, the fracture performance tends to be anisotropic. The geometric and morphological characteristics (such as aspect ratio and orientation angle) of aggregates affect the fracture pattern and the damage level when the tension is applied in two orthogonal directions.
4. Large aggregate size proves to pose a negative effect on the fracture performance of asphalt concrete. When the total aggregate content is the same, the large aggregate in asphalt concrete raise the heterogeneity level between different aggregate sizes which increases interface damage and stress concentration. Large aggregates contribute more to the structure stiffness yet they may bring challenge into the fracture performance design.

5.2 Findings on Simulation of Asphalt Concrete in Semi-Circular Bending Test

1. The heterogeneous model with viscoelastic behavior was successful in simulating fracture behavior of asphalt concrete at different temperatures and loading rates. The simulation results fit well with the test data reported in the literature. Compared to the low temperature, more energy dissipates at high temperature due to material viscoelasticity. At the low temperature, asphalt concrete tends to

behave as an elastic material; loading rate does not significantly affect the fracture energy of asphalt concrete.

2. The randomly generated microstructure proves to be reasonable in modeling aggregate distribution within the asphalt concrete. The distribution and angularity of coarse aggregate have an influence on crack path; but the overall fracture resistance does not change much when asphalt concrete samples are prepared using the same aggregate gradation. On the other hand, the gradation and size of coarse aggregate have considerable effects on the fracture strength and accordingly fracture energy of asphalt concrete.
3. Increasing fracture strength and fracture energy of the FAM material significantly improves fracture resistance of asphalt concrete. The higher fracture strength results in the greater peak load while the higher fracture energy would slow down the damage process by requiring more energy for the crack to propagate.
4. The results indicate that the fracture behavior of asphalt concrete can be effectively predicted with viscoelastic and fracture parameters of FAM material and coarse aggregate gradation. Improvement is needed in future research to take into consideration the effect of aggregate-FAM interaction and air voids on fracture resistance of asphalt concrete.

5.3 Recommendation for Future Work

Despite the advanced finite element model utilized in this study, several improvements can be done to better model fracture behavior of asphalt concrete numerically:

1. This study accounted for the heterogeneous effect by modeling asphalt concrete as a two-phase material and an interface. As asphalt binder and aggregates are not

the only factors affecting the fracture performance of asphalt concrete, in order to build the more accurate microstructure, other phases could be added into the model such as air void and other additives.

2. The microstructure models used in this study have uniform aggregate morphological parameters (angularity index, aspect ratio, and edges of polygon) representing the aggregate morphology within an individual digital specimen. In real asphalt concrete, the aggregates have various morphological parameters. A better random generation algorithm is needed to more realistically produce the microstructure sample for numerical analysis.
3. The numerical models considered coarse aggregates only for the aggregate phase; while fine aggregates were combined with binder in the FAM. The influence of fine aggregates on fracture behavior need to be investigated in the future. It will require a more complicated modeling technique and higher computation costs.

REFERENCE

ABAQUS. (2010) ABAQUS analysis user's manual, version 6.10. Pawtucket, RI, USA: Habbit, Karlsson & Sorenson Inc.

Allen, R. G., Little, D. N., Bhasin, A., & Lytton, R. L. (2012). Identification of the composite relaxation modulus of asphalt binder using AFM nanoindentation. *Journal of Materials in Civil Engineering*, 25(4), 530-539.

Anderson T.L. (1995) Fracture Mechanics - Fundamental and Applications, CRC Press.

Aragão FTS, Hartmann DA, Kim YR, da Motta LMG, Javaherian MH.(2014) Numerical–experimental approach to characterize fracture properties of asphalt mixtures at low in-service temperatures. In: *Proceeding of transportation research board 93rd annual meeting*; [paper # 14-4905].

Aragão, F. T. S., Kim, Y. R., Lee, J., & Allen, D. H. (2010). Micromechanical model for heterogeneous asphalt concrete mixtures subjected to fracture failure. *Journal of Materials in Civil Engineering*, 23(1), 30-38.

Babuska, I., & Melenk, J. M. (1995). The partition of unity finite element method (No. TN-BN-1185). MARYLAND UNIV COLLEGE PARK INST FOR PHYSICAL SCIENCE AND TECHNOLOGY.

Barenblatt, G. I. (1962). The mathematical theory of equilibrium cracks in brittle fracture. *Advances in applied mechanics*, 7(1), 55-129.

Bazant, Z. P., Tabbara, M. R., Kazemi, M. T., & Pijaudier-Cabot, G. (1990). Random particle model for fracture of aggregate or fiber composites. *Journal of Engineering Mechanics*, 116(8), 1686-1705.

Belytschko, T., & Black, T. (1999). Elastic crack growth in finite elements with minimal remeshing. *International journal for numerical methods in engineering*, 45(5), 601-620.

Brzezicki, J. M., & Kasperkiewicz, J. (1999). Automatic image analysis in evaluation of aggregate shape. *Journal of Computing in Civil Engineering*, 13(2), 123-128.

Chen, J., Pan, T., & Huang, X. (2011). Numerical investigation into the stiffness anisotropy of asphalt concrete from a microstructural perspective. *Construction and Building Materials*, 25(7), 3059-3065.

Dai, Q., Sadd, M. H., Parameswaran, V., & Shukla, A. (2005). Prediction of damage behaviors in asphalt materials using a micromechanical finite-element model and image analysis. *Journal of Engineering Mechanics*, 131(7), 668-677.

De Schutter, G., & Taerwe, L. (1993). Random particle model for concrete based on Delaunay triangulation. *Materials and Structures*, 26(2), 67-73.

de Souza, F. V., Soares, J. B., Allen, D. H., & Evangelista, F. (2004). Model for predicting damage evolution in heterogeneous viscoelastic asphaltic mixtures. *Transportation Research Record: Journal of the Transportation Research Board*, 1891(1), 131-139.

Du, X., Jin, L., & Ma, G. (2013). Numerical modeling tensile failure behavior of concrete at mesoscale using extended finite element method. *International Journal of Damage Mechanics*, 1056789513516028.

Dugdale, D. S. (1960). Yielding of steel sheets containing slits. *Journal of the Mechanics and Physics of Solids*, 8(2), 100-104.

Elseifi, M. A., Mohammad, L. N., Ying, H., & Cooper III, S. (2012). Modeling and evaluation of the cracking resistance of asphalt mixtures using the semi-circular bending test at intermediate temperatures. *Road Materials and Pavement Design*, 13(sup1), 124-139.

Ferry, J. D. (1980). Viscoelastic properties of polymers. John Wiley & Sons.

Fini, E. H., & Al-Qadi, I. L. (2011). Development of a pressurized blister test for interface characterization of aggregate highly polymerized bituminous materials. *Journal of materials in civil engineering*, 23(5), 656-663.

Griffith, A. A. (1921). The phenomena of rupture and flow in solids. *Philosophical transactions of the royal society of london. Series A, containing papers of a mathematical or physical character*, 163-198.

Guddati, M. N., Feng, Z., & Kim, Y. R. (2002). Toward a micromechanics-based procedure to characterize fatigue performance of asphalt concrete. *Transportation Research Record: Journal of the Transportation Research Board*, 1789(1), 121-128.

Hillerborg, A., Modéer, M., & Petersson, P. E. (1976). Analysis of crack formation and crack growth in concrete by means of fracture mechanics and finite elements. *Cement and concrete research*, 6(6), 773-781.

Hoare, T.R., Hesp, S.A.M. (2000). “Low-temperature fracture testing of asphalt binders: regular and modified systems.” *Transportation Research Record*, 1728:36–42

Im, S. (2012) Characterization of Viscoelastic and Fracture Properties of Asphaltic Materials in Multiple Length Scales. *PhD Dissertation, University of Nebraska – Lincoln*.

Irwin, G. R. (1957). Analysis of stresses and strains near the end of a crack traversing a plate. *J. appl. Mech.*

Khattak, M. J., Baladi, G. Y., & Drzal, L. T. (2007). Low temperature binder-aggregate adhesion and mechanistic characteristics of polymer modified asphalt mixtures. *Journal of materials in civil engineering*, 19(5), 411-422.

Kim, H., Wagoner, M. P., & Buttlar, W. G. (2008). Simulation of fracture behavior in asphalt concrete using a heterogeneous cohesive zone discrete element model. *Journal of Materials in Civil Engineering*, 20(8), 552-563.

Kim, H. and Buttlar, W.G. (2009). “Discrete Fracture Modeling of Asphalt Concrete. *International Journal of Solids and Structures*, 46, 2593-2604.

Kim, K.W., Kweon S.J., Doh, Y.S., and Park, T.S. (2003). “Fracture toughness of polymer-modified asphalt concrete at low temperatures.” *Canadian Journal of Civil Engineering*, 30, 406-413.

Kim, S. M., & Abu Al-Rub, R. K. (2011). Meso-scale computational modeling of the plastic-damage response of cementitious composites. *Cement and Concrete Research*, 41(3), 339-358.

Kim, Y. R., Allen, D. H., & Little, D. N. (2005). Damage-induced modeling of asphalt mixtures through computational micromechanics and cohesive zone fracture. *Journal of Materials in Civil Engineering*, 17(5), 477-484.

Kim, Y.R., Allen, D.H., and Little, D.N., (2007). "Computational constitutive model for predicting nonlinear viscoelastic damage and fracture failure of asphalt concrete mixtures." *International Journal of Geomechanics*, 7(2), 102-110.

Kim, Y. R., & Aragão, F. T. S. (2013). Microstructure modeling of rate-dependent fracture behavior in bituminous paving mixtures. *Finite Elements in Analysis and Design*, 63, 23-32.

Kristiansen, K. D. L., Wouterse, A., & Philipse, A. (2005). Simulation of random packing of binary sphere mixtures by mechanical contraction. *Physica A: Statistical Mechanics and its Applications*, 358(2), 249-262.

Kuo, C. Y., Frost, J. D., Lai, J. S., & Wang, L. B. (1996). Three-dimensional image analysis of aggregate particles from orthogonal projections. *Transportation Research Record: Journal of the Transportation Research Board*, 1526(1), 98-103.

Lancaster, I. M., Khalid, H. A., & Kougioumtzoglou, I. A. (2013). Extended FEM modelling of crack propagation using the semi-circular bending test. *Construction and Building Materials*, 48, 270-277.

Lee, N.K, Morrison, G.R., and Hesp S.A.M. (1995). “Low temperature fracture of polyethylene-modified asphalt binders and asphalt concrete mixes.” *Journal of the Association of Asphalt Paving Technologists*, 64:534–574

Li, X., & Marasteanu, M. (2004). Evaluation of the low temperature fracture resistance of asphalt mixtures using the semi circular bend test (with discussion). *Journal of the Association of Asphalt Paving Technologists*, 73.

Li, X., & Marasteanu, M. O. (2006). Investigation of low temperature cracking in asphalt mixtures by acoustic emission. *Road materials and pavement design*, 7(4), 491-512.

Mahmoud, E., Saadeh, S., Hakimelahi, H., & Harvey, J. (2014). Extended finite-element modelling of asphalt mixtures fracture properties using the semi-circular bending test. *Road Materials and Pavement Design*, 15(1), 153-166.

Marasteanu, M.O., Dai, S.T., Labuz, J.F., and Li, X. (2002). “Determining the low-temperature fracture toughness of asphalt mixtures.” *Transportation Research Record* 1789, 191-199.

Masad, E., Muhunthan, B., Shashidhar, N., & Harman, T. (1999). Internal structure characterization of asphalt concrete using image analysis. *Journal of computing in civil engineering*, 13(2), 88-95.

Masad, E., Button, J. W., & Papagiannakis, T. (2000). Fine-aggregate angularity: automated image analysis approach. *Transportation Research Record: Journal of the Transportation Research Board*, 1721(1), 66-72.

Masad, E., Olcott, D., White, T., & Tashman, L. (2001). Correlation of fine aggregate imaging shape indices with asphalt mixture performance. *Transportation Research Record: Journal of the Transportation Research Board*, 1757(1), 148-156.

Masad, E., Tashman, L., Somedavan, N., & Little, D. (2002). Micromechanics-based analysis of stiffness anisotropy in asphalt mixtures. *Journal of Materials in Civil Engineering*, 14(5), 374-383

Mobasher, B., Mamlouk, M., and Lin, H. (1997). "Evaluation of crack propagation properties of asphalt mixtures." *Journal of Transportation Engineering*, 123 (5):405–413.

Molenaar, A. A. A., Scarpas, A., Liu, X., & Erkens, S. M. J. G. (2002). Semi-circular bending test; simple but useful?. *Journal of the Association of Asphalt Paving Technologists*, 71.

Mull, M.A., Stuart, K., and Yehia, A. (2002). "Fracture resistance characterization of chemically modified crumb rubber asphalt pavement." *Journal of Materials Science*, 37, 557-566

Ng, K., & Dai, Q. (2011). Tailored Extended Finite-Element Model for Predicting Crack Propagation and Fracture Properties within Idealized and Digital Cementitious Material Samples. *Journal of Engineering Mechanics*, 138(1), 89-100.

Ng, K., & Dai, Q. (2011). Investigation of fracture behavior of heterogeneous infrastructure materials with extended-finite-element method and image analysis. *Journal of Materials in Civil Engineering*, 23(12), 1662-1671.

Osher, S., & Fedkiw, R. P. (2001). Level set methods: an overview and some recent results. *Journal of Computational physics*, 169(2), 463-502.

Rao, C., Tutumluer, E., & Kim, I. T. (2002). Quantification of coarse aggregate angularity based on image analysis. *Transportation Research Record: Journal of the Transportation Research Board*, 1787(1), 117-124.

Sadd, M. H., Dai, Q., Parameswaran, V., & Shukla, A. (2004). Microstructural simulation of asphalt materials: modeling and experimental studies. *Journal of materials in civil engineering*, 16(2), 107-115.

Sánchez-Leal, F. J. (2007). Gradation chart for asphalt mixes: Development. *Journal of Materials in Civil Engineering*, 19(2), 185-197.

Seo, Y. G. (2003) A Comprehensive Study of Crack Growth in Asphalt Concrete Using Fracture Mechanics. *Ph.D. Dissertation, Civil Engineering, North Carolina State University*.

Seyhan, U., & Tutumluer, E. (2002). Anisotropic modular ratios as unbound aggregate performance indicators. *Journal of Materials in Civil Engineering*, 14(5), 409-416.

Soares, J. B., Freitas, F. A., & Allen, D. H. (2003). Crack modeling of asphaltic mixtures considering heterogeneity of the material. *Transp. Res. Rec*, 1832, 113-120.

Song, S. H., Paulino, G. H., & Buttlar, W. G. (2006). A bilinear cohesive zone model tailored for fracture of asphalt concrete considering viscoelastic bulk material. *Engineering Fracture Mechanics*, 73(18), 2829-2848.

Souza, L. T., Kim, Y. R., Souza, F. V., & Castro, L. S. (2012). Experimental testing and finite-element modeling to evaluate the effects of aggregate angularity on bituminous mixture performance. *Journal of Materials in Civil Engineering*, 24(3), 249-258.

Tarefder, R., & Faisal, H. (2013). Nanoindentation characterization of asphalt concrete aging. *Journal of Nanomechanics and Micromechanics*, 4(1).

Tarrer, A. R., & Wagh, V. (1991). The effect of the physical and chemical characteristics of the aggregate on bonding (No. SHRP-A/UIR-91-507). Washington, DC: Strategic Highway Research Program, National Research Council.

Tutumluer, E., Adu-Osei, A., Little, D. N., & Lytton, R. L. (2001). *Field validation of the cross-anisotropic behavior of unbound aggregate bases* (No. ICAR-502-2). International Center for Aggregates Research.

Tschoegl, N. W., & Tschoegl, N. W. (1989). The phenomenological theory of linear viscoelastic behavior: an introduction (pp. 143-145). Berlin: Springer-Verlag.

Underwood, S., Heidari, A. H., Guddati, M., & Kim, Y. R. (2005). Experimental investigation of anisotropy in asphalt concrete. *Transportation Research Record: Journal of the Transportation Research Board*, 1929(1), 238-247.

Wagoner, M. P., Buttlar, W. G., & Paulino, G. H. (2005). Development of a single-edge notched beam test for asphalt concrete mixtures. *Journal of Testing and Evaluation*, 33(6), 452.

Wagnoner, M. P., Buttlar, W. G., & Paulino, G. H. (2005). Disk-shaped compact tension test for asphalt concrete fracture. *Experimental Mechanics*, 45(3), 270-277.

Wagoner, M. P., Buttlar, W. G., Paulino, G. H., & Blankenship, P. (2006). Laboratory Testing Suite for Characterization of Asphalt Concrete Mixtures Obtained from Field Cores (With Discussion). *Journal of the Association of Asphalt Paving Technologists*, 75.

Wagoner, M.P. (2006). Fracture Tests for Bituminous-Aggregates Mixtures: Laboratory and Field Investigations. *Ph.D. Dissertation, University of Illinois*. Urbana, Illinois.

Wang, D., Wang, L., Druta, C., Xue, W., Xiong, H., & Sun, W. (2013). Experimental Evaluation of a Simple Contact Model Containing Two Elastic Particles Bonded by a Thin Layer of Viscoelastic Binder. *Journal of Nanomechanics and Micromechanics*, 3(4).

Wang, H., Wang, J., & Chen, J. (2014). Micromechanical Analysis of Asphalt Mixture Fracture with Adhesive and Cohesive Failure. *Engineering Fracture Mechanics*.

Wang, L., Wang, X., Mohammad, L., & Abadie, C. (2005). Unified method to quantify aggregate shape angularity and texture using Fourier analysis. *Journal of Materials in Civil Engineering*, 17(5), 498-504.

Wang, L., Hoyos, L. R., Wang, J., Voyiadjis, G., & Abadie, C. (2005). Anisotropic properties of asphalt concrete: Characterization and implications for pavement design and analysis. *Journal of materials in civil engineering*, 17(5), 535-543.

Wang, Z. M., Kwan, A. K. H., & Chan, H. C. (1999). Mesoscopic study of concrete I: generation of random aggregate structure and finite element mesh. *Computers & structures*, 70(5), 533-544.

Wittmann, F. H., Roelfstra, P. E., & Sadouki, H. (1985). Simulation and analysis of composite structures. *Materials science and engineering*, 68(2), 239-248.

Xie, D., & Biggers Jr, S. B. (2006). Progressive crack growth analysis using interface element based on the virtual crack closure technique. *Finite Elements in Analysis and Design*, 42(11), 977-984.

Yin, A., Yang, X., Gao, H., & Zhu, H. (2012). Tensile fracture simulation of random heterogeneous asphalt mixture with cohesive crack model. *Engineering Fracture Mechanics*, 92, 40-55.

Zhang, Y., Luo, R., & Lytton, R. L. (2011). Anisotropic viscoelastic properties of undamaged asphalt mixtures. *Journal of Transportation Engineering*, 138(1), 75-89.